

Drug Discovery II

Arthur G. Roberts

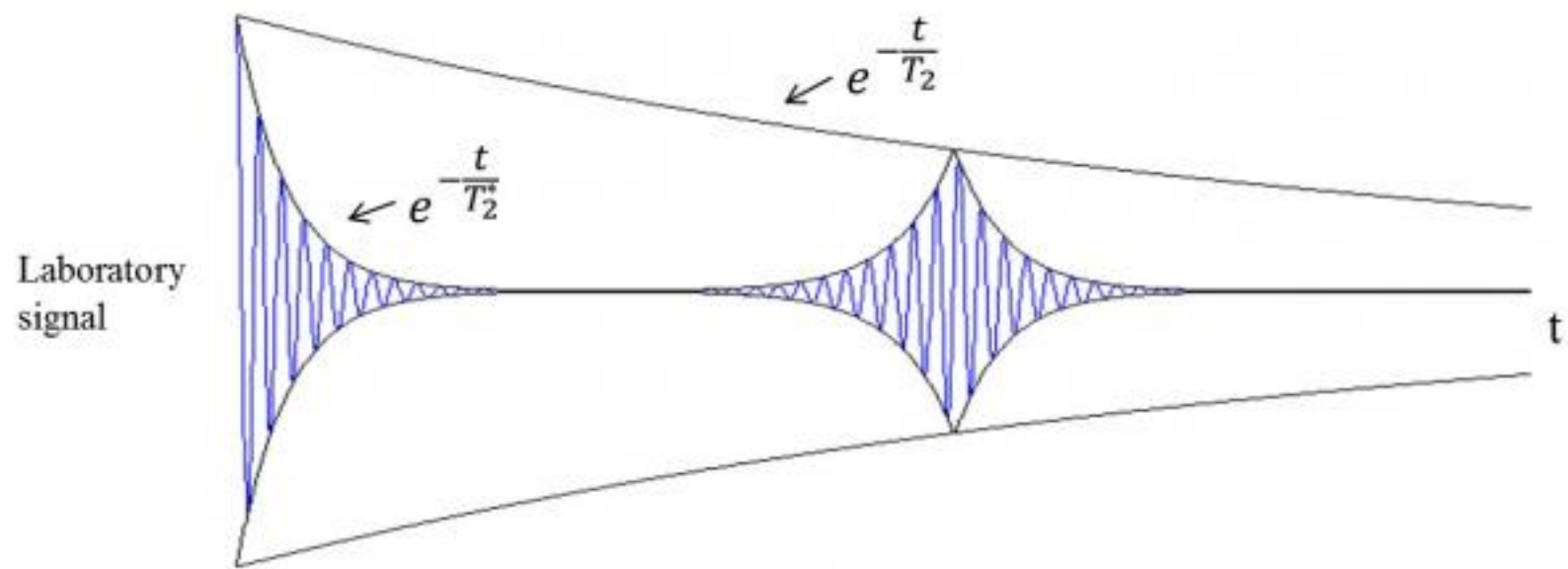
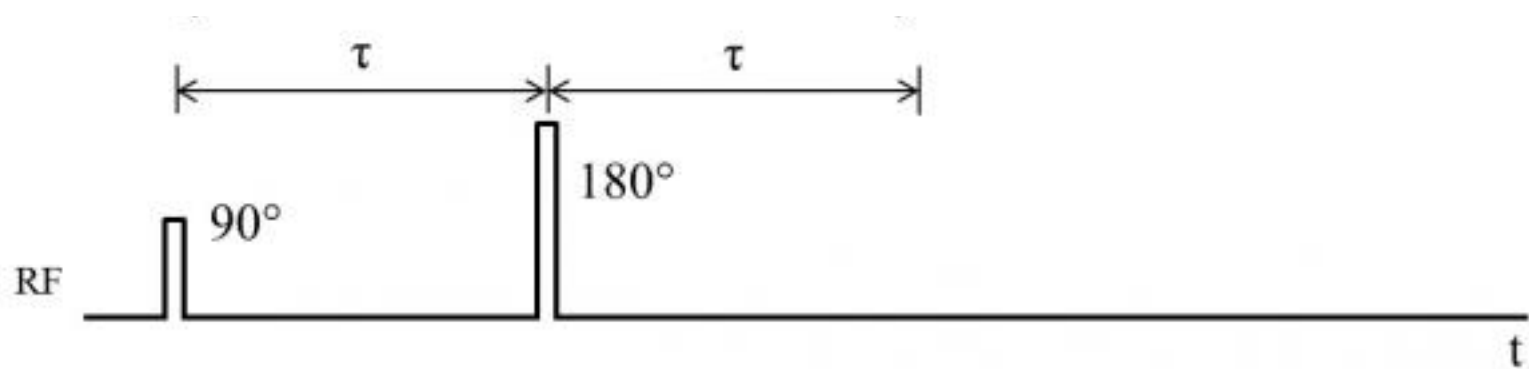
Ligand-based NMR Screening

- **Chemical Shift**
- **Saturation Transfer Difference**
- **Relaxation Methods**
- **Diffusion Editing**
- NOE-based Methods
- Residual Dipolar Couplings
- Other

Diffusion NMR

- Self Diffusion (SD)-NMR
- Diffusion Ordered Spectroscopy (DOSY)

Spin Echo



Field Gradient

Magnetic Field

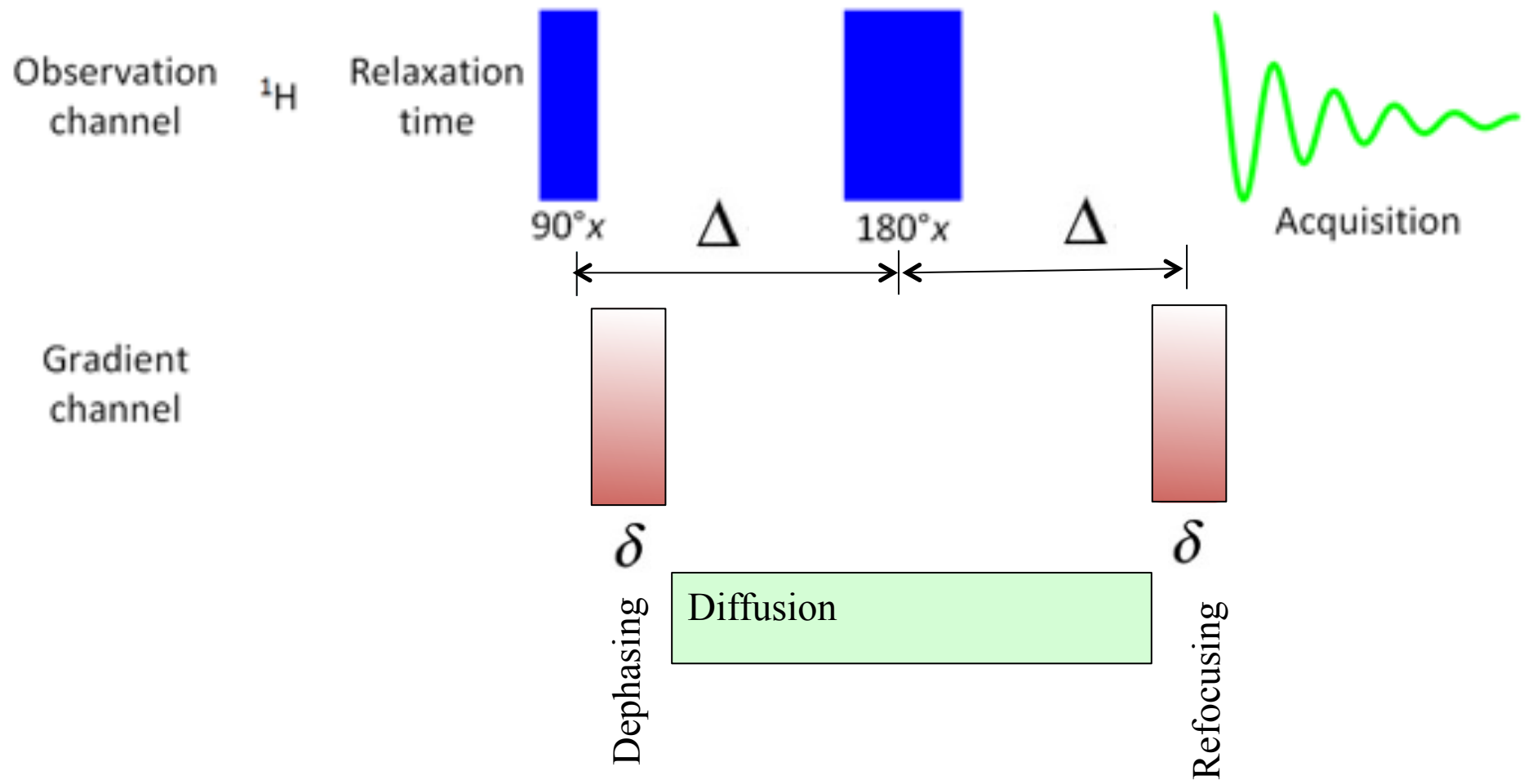
Weaker



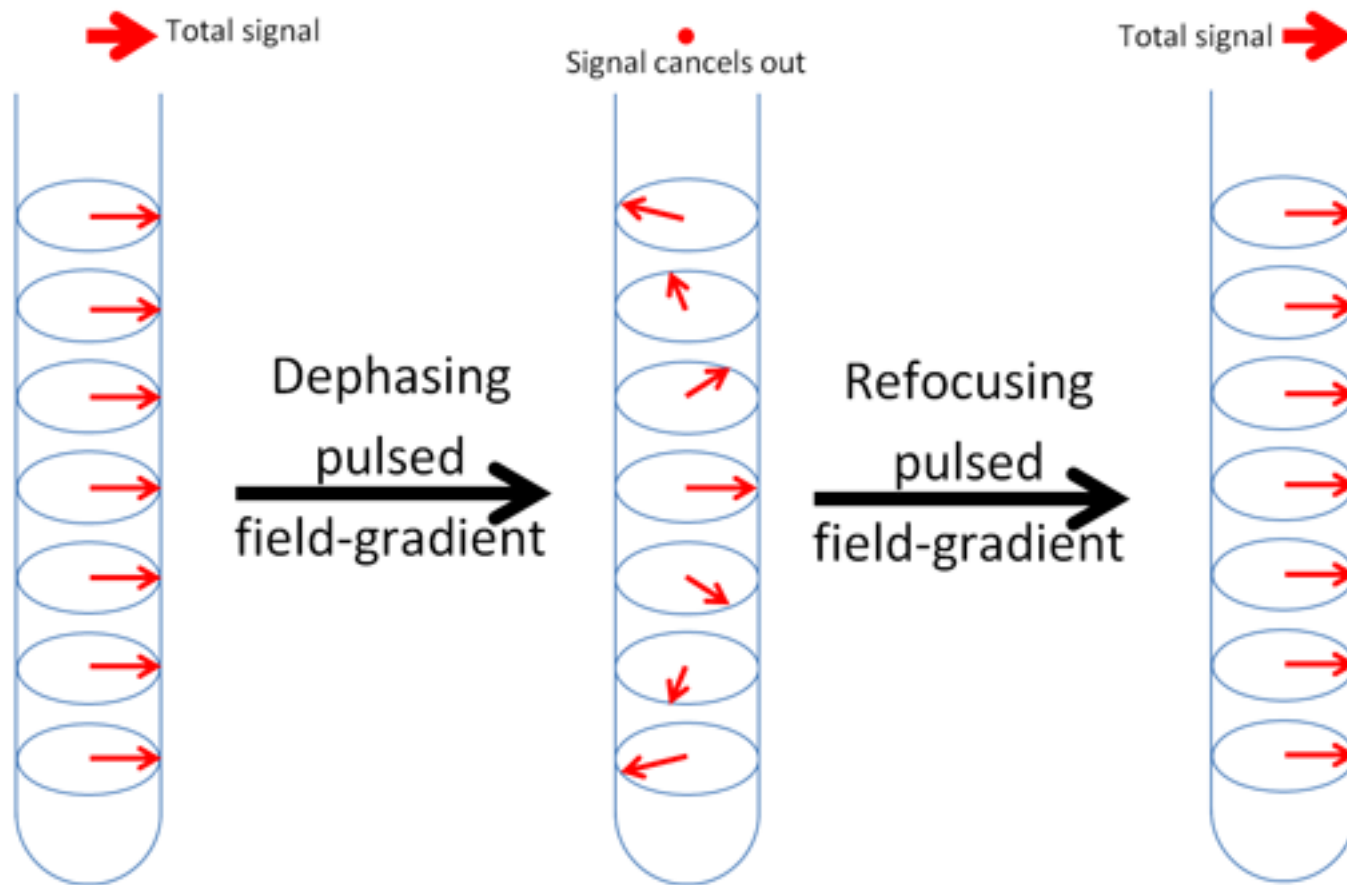
Magnetization in Tube



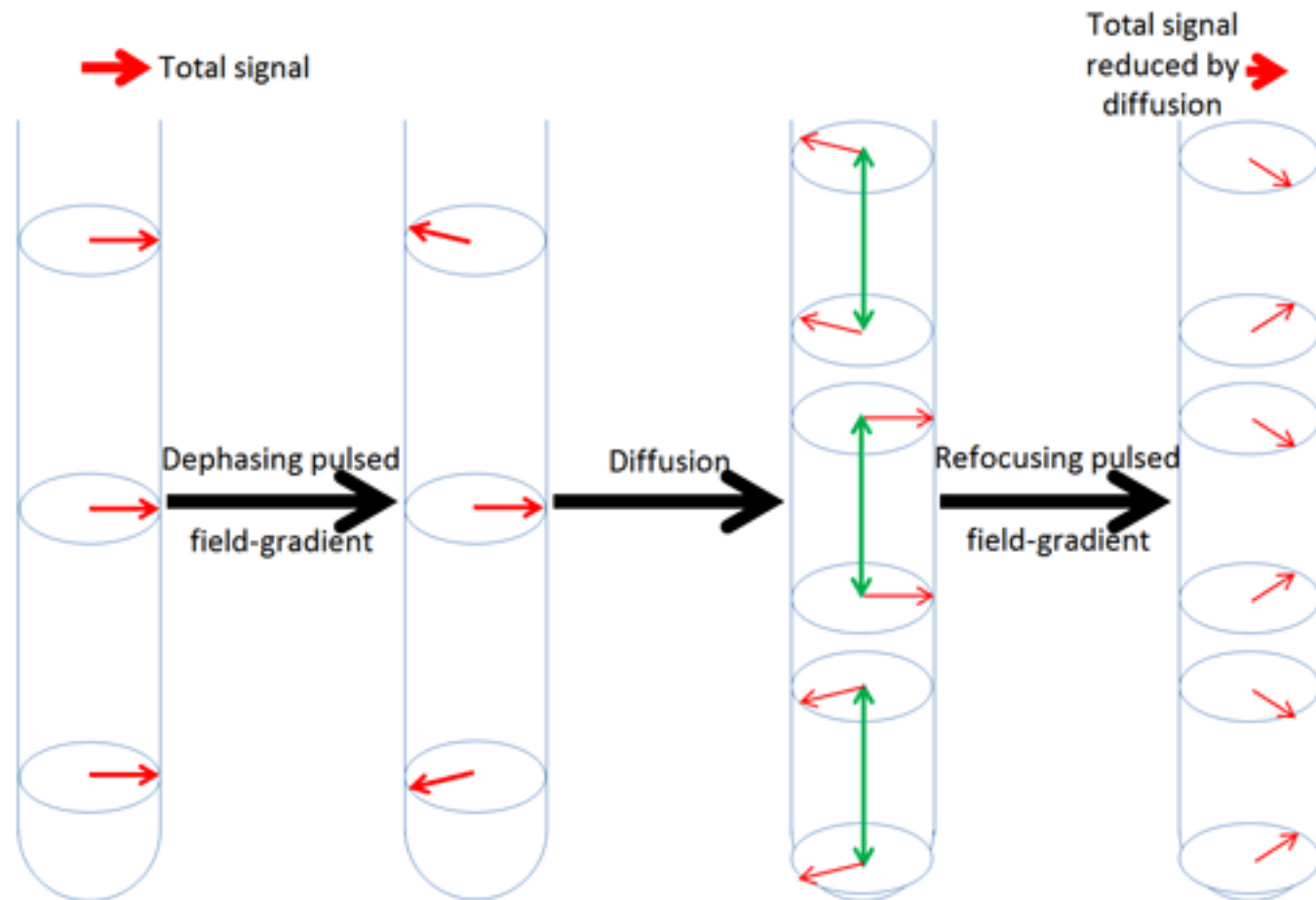
Pulsed Field Gradient Spin Echo (PGSE)



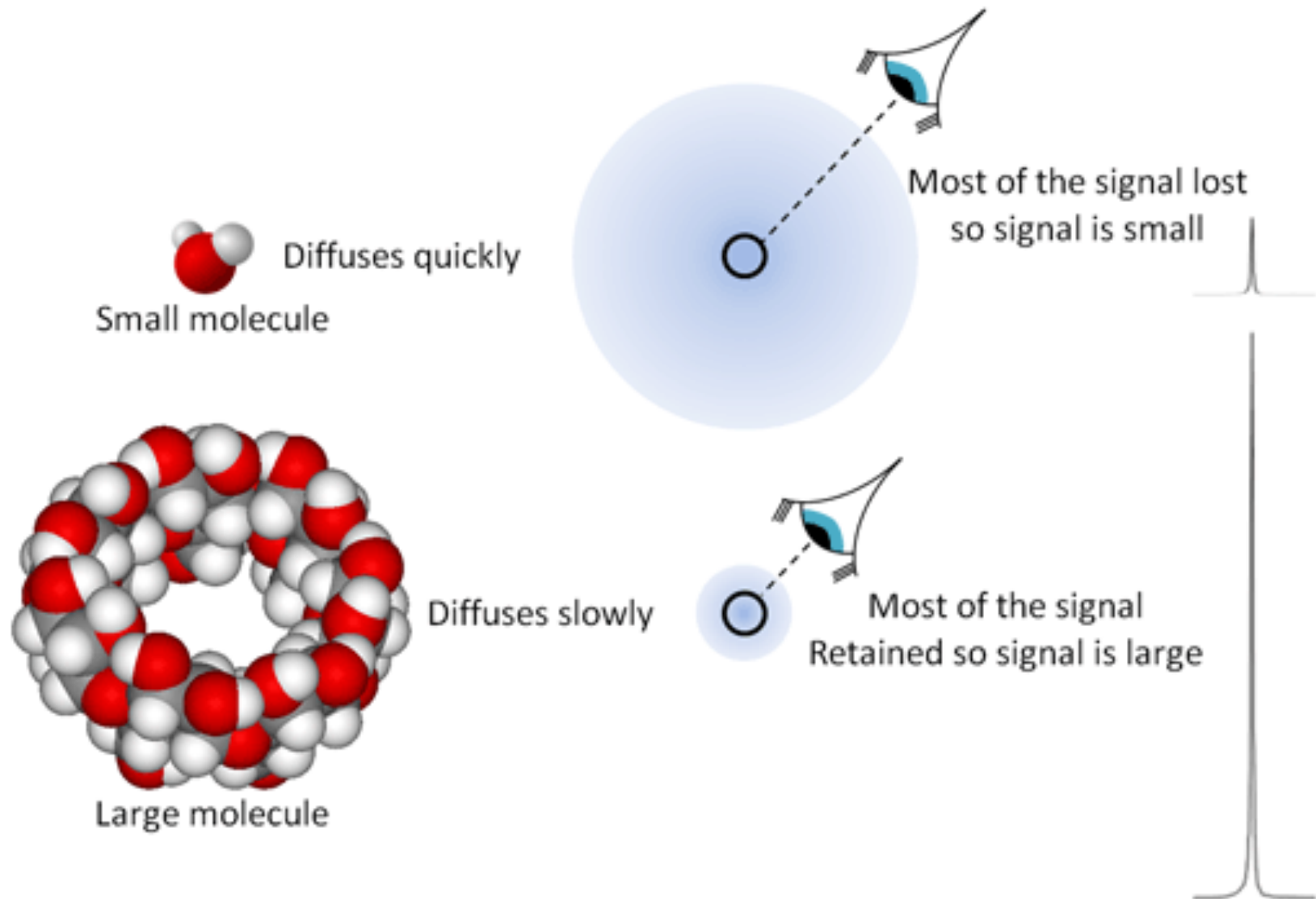
Pulsed Field Gradient Spin Echo (PGSE): No Diffusion



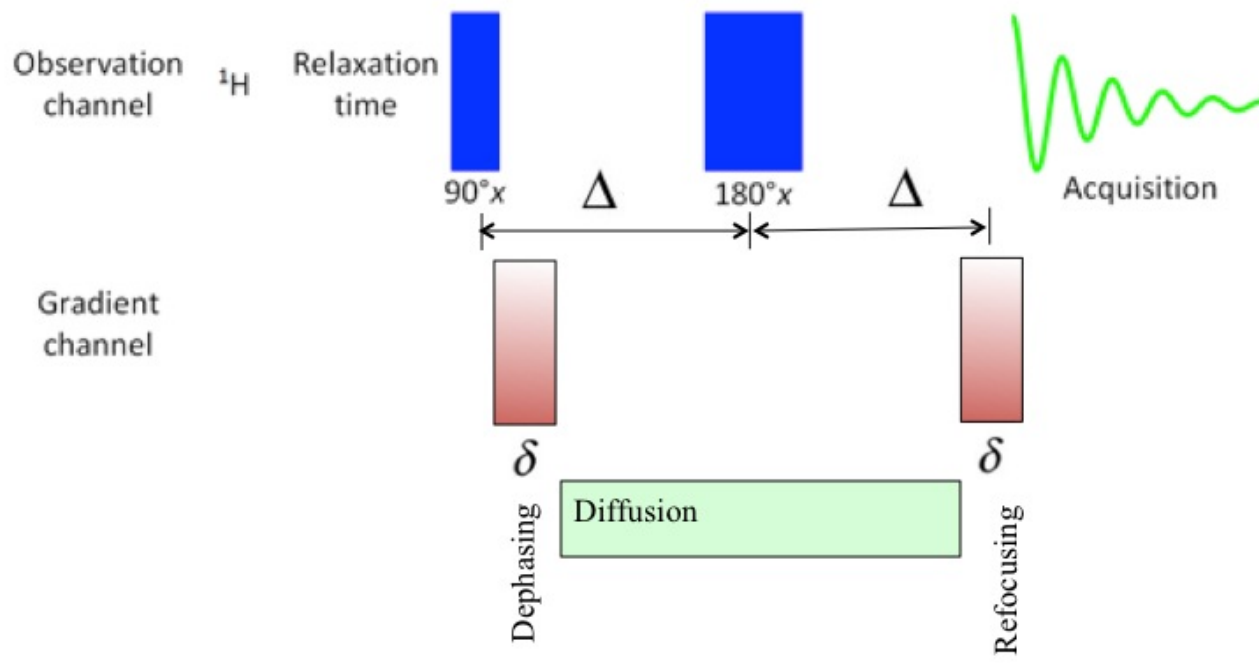
Pulsed Field Gradient Spin Echo (PGSE): Diffusion



Pulsed Field Gradient Spin Echo (PGSE): Diffusion



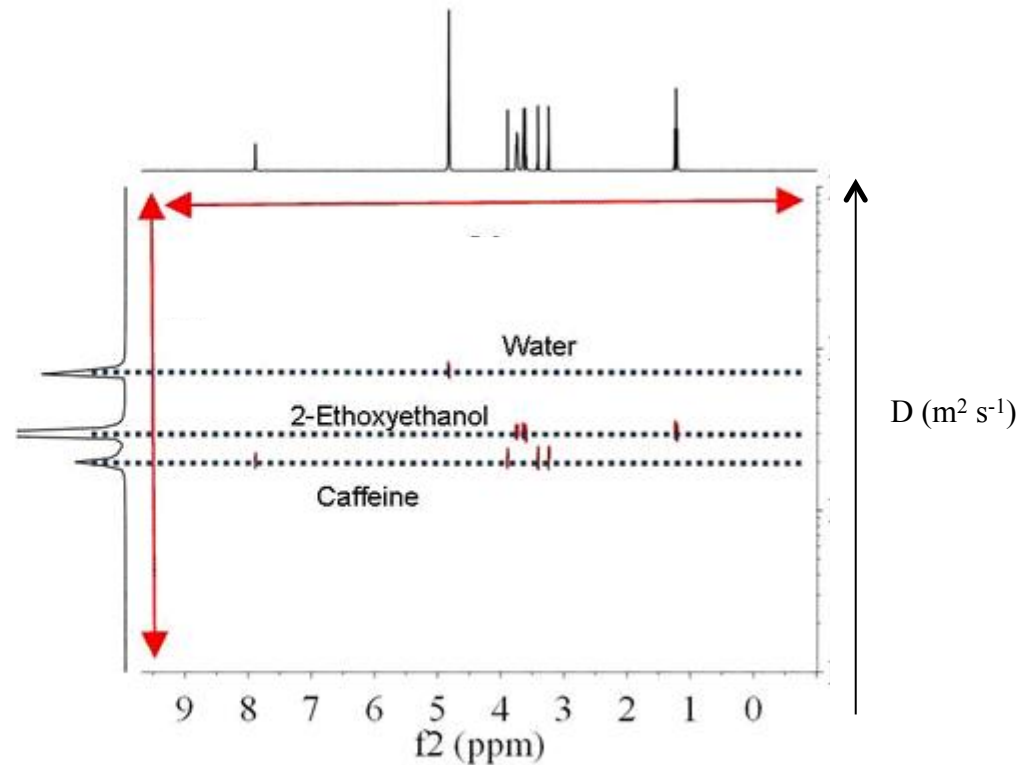
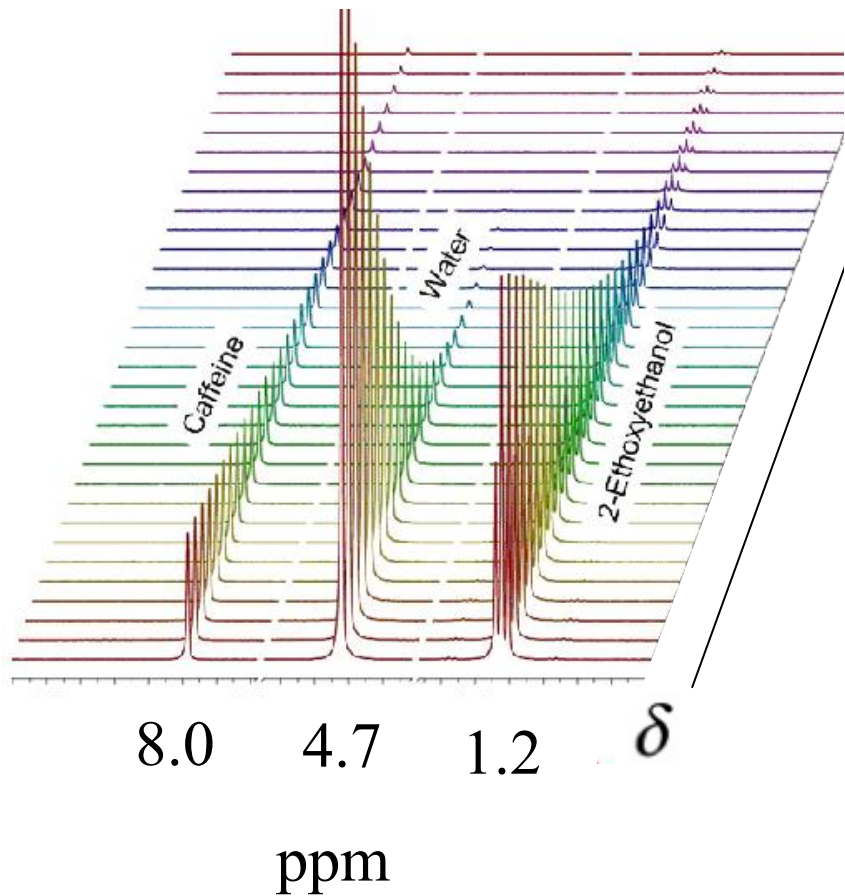
Pulsed Field Gradient Spin Echo (PGSE)



$$\begin{array}{ll} \gamma & \text{gyromagnetic ratio (rad s}^{-1} \text{ T}^{-1}\text{)} \\ g & \text{g-factor (unitless)} \\ D & \text{diffusion constant (m}^2 \text{ s}^{-1}\text{)} \end{array} \quad I = \exp \left[-(\gamma \cdot g \cdot \delta)^2 D \cdot \left(2 \cdot \Delta - \frac{\delta}{3} \right) \right]$$

Diffusion NMR can be used to separate a mixture.

Mixture



Diffusion Edited Screening

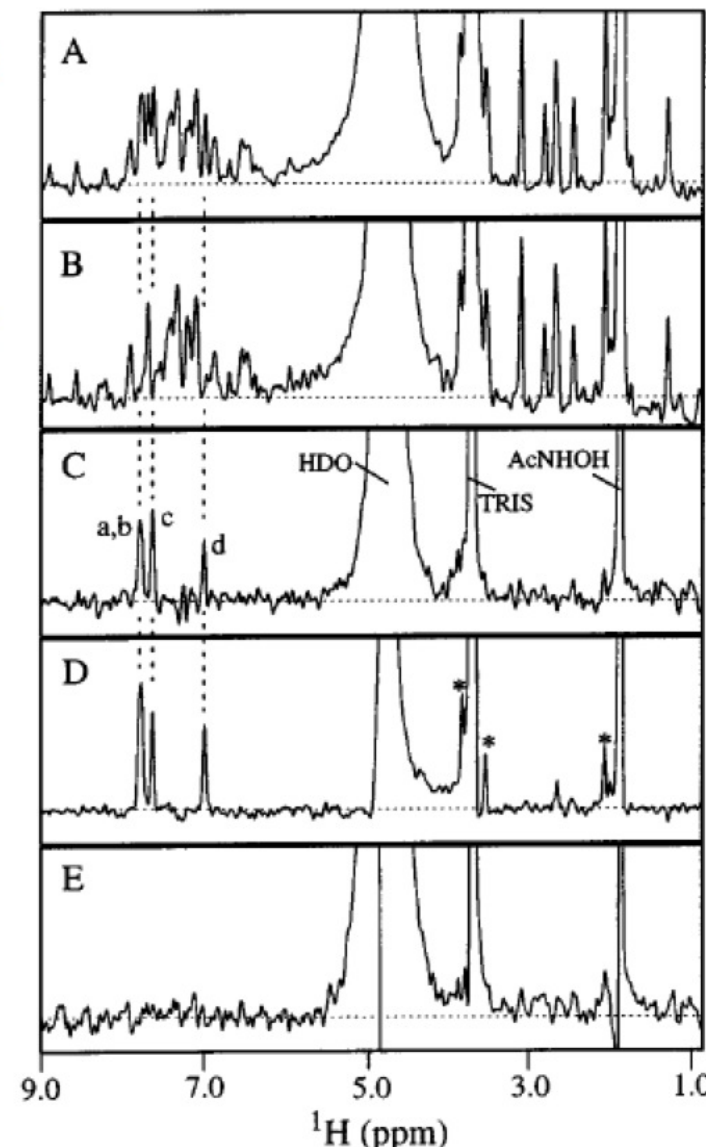
**Compound Mixture alone
in the presence of
gradient**

**Compound Mixture plus
protein in the presence of
gradient**

Spectra (A) minus Spectra (B).
**Difference only occurs if the
diffusion of a compound has
changed**

**Free compound in
(c)**

**Protein and buffer
reference**



Diffusion editing to demonstrate that 4-cyano-4' hydroxybiphenyl, which binds to stromelysin with a dissociation constant of 20 μ M, was easily identified from a mixture containing eight other non-binding compounds.

Analysis of ligand binding to the catalytic domain of stromelysin by using a diffusion-edited approach. (A) PFG-STE spectrum of a mixture of nine compounds (2-10) in the absence of stromelysin with use of low gradient strengths. (B) PFG-STE spectrum of a mixture of nine compounds (2-10) in the presence of stromelysin with use of a low-gradient strength, after removal of protein signals by subtracting a PFG-STE spectrum of the same sample obtained at high gradient strengths. (C) A difference spectrum obtained by subtracting the spectrum in B from that in A. (D) A reference spectrum of 2 alone. (E) A difference spectrum obtained in an analogous fashion to the spectrum shown in C, but on a mixture of eight compounds (3-10) which do not bind to stromelysin.

Diffusion Edited Screening Example

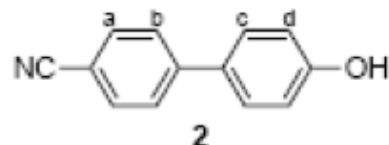
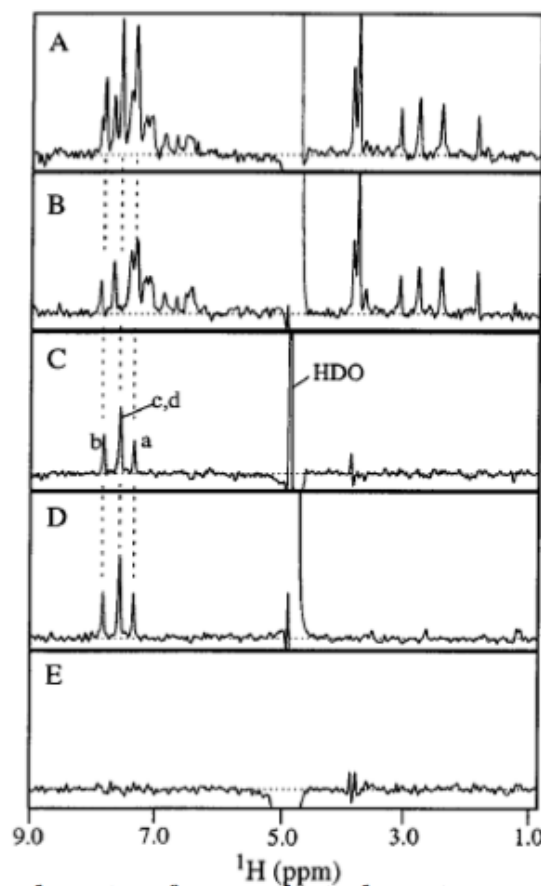


Table 1. Inactive Compounds^a Tested Against FKBP and Stromelysin

Compound No.	Structure
3	
4	
5	
6	
7	
8	
9	
10	



Hajduk, P. J., E. T. Olejniczak and S. W. Fesik (1997). "One-dimensional relaxation- and diffusion-edited NMR methods for screening compounds that bind to macromolecules." *Journal of the American Chemical Society* **119**(50): 12257-12261.

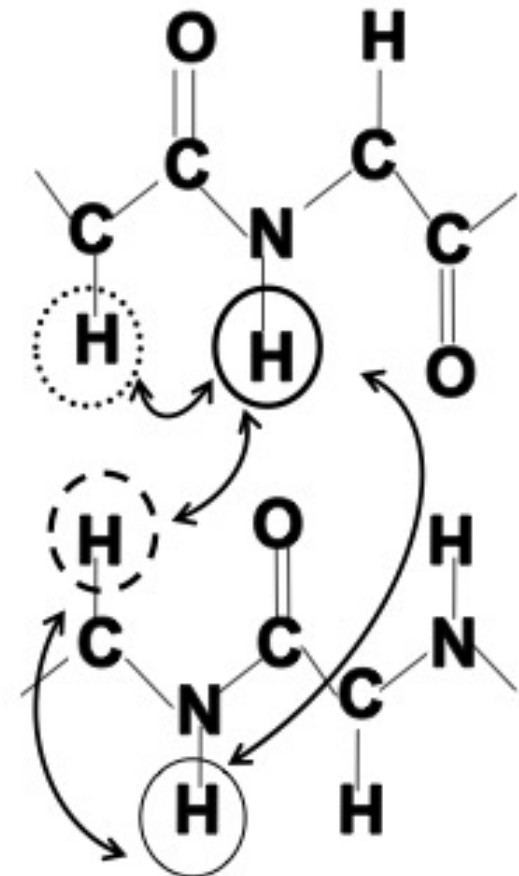
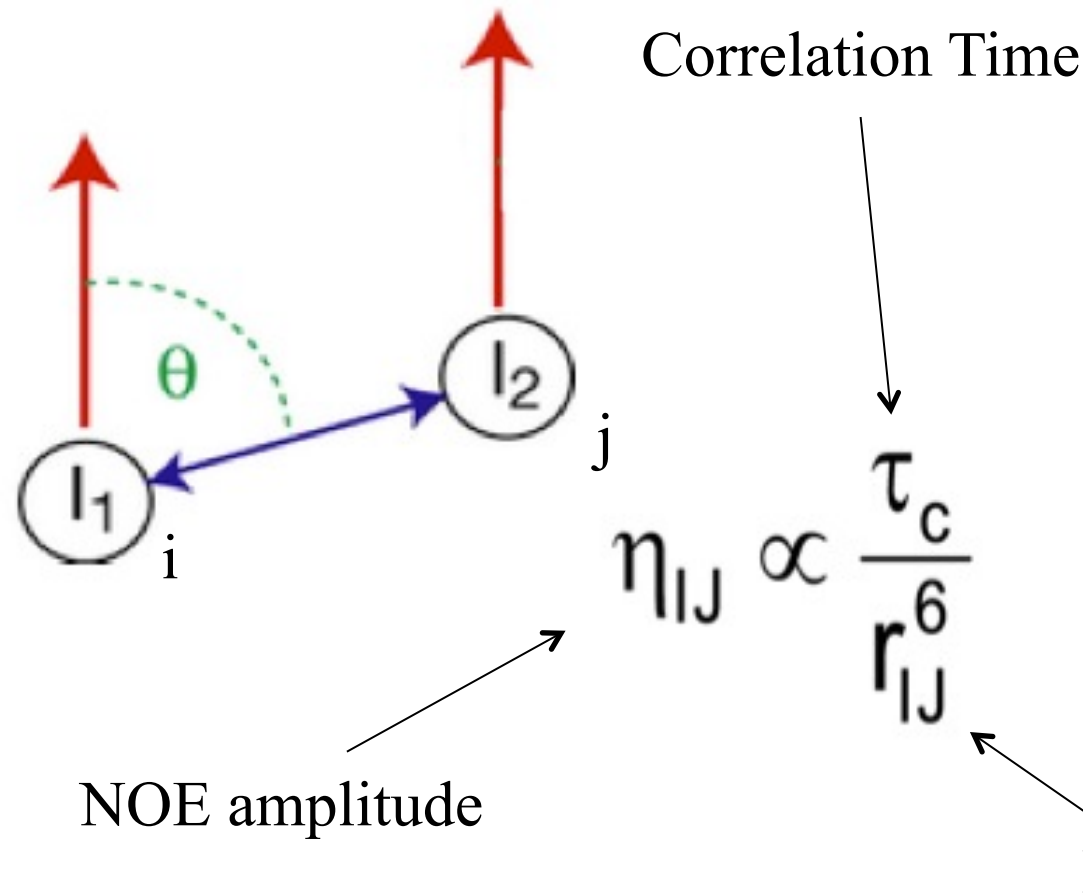
Ligand-based NMR Screening

- **Chemical Shift**
- **Saturation Transfer Difference**
- **Relaxation Methods**
- **Diffusion Editing**
- **NOE-based Methods**
- Residual Dipolar Couplings
- Other

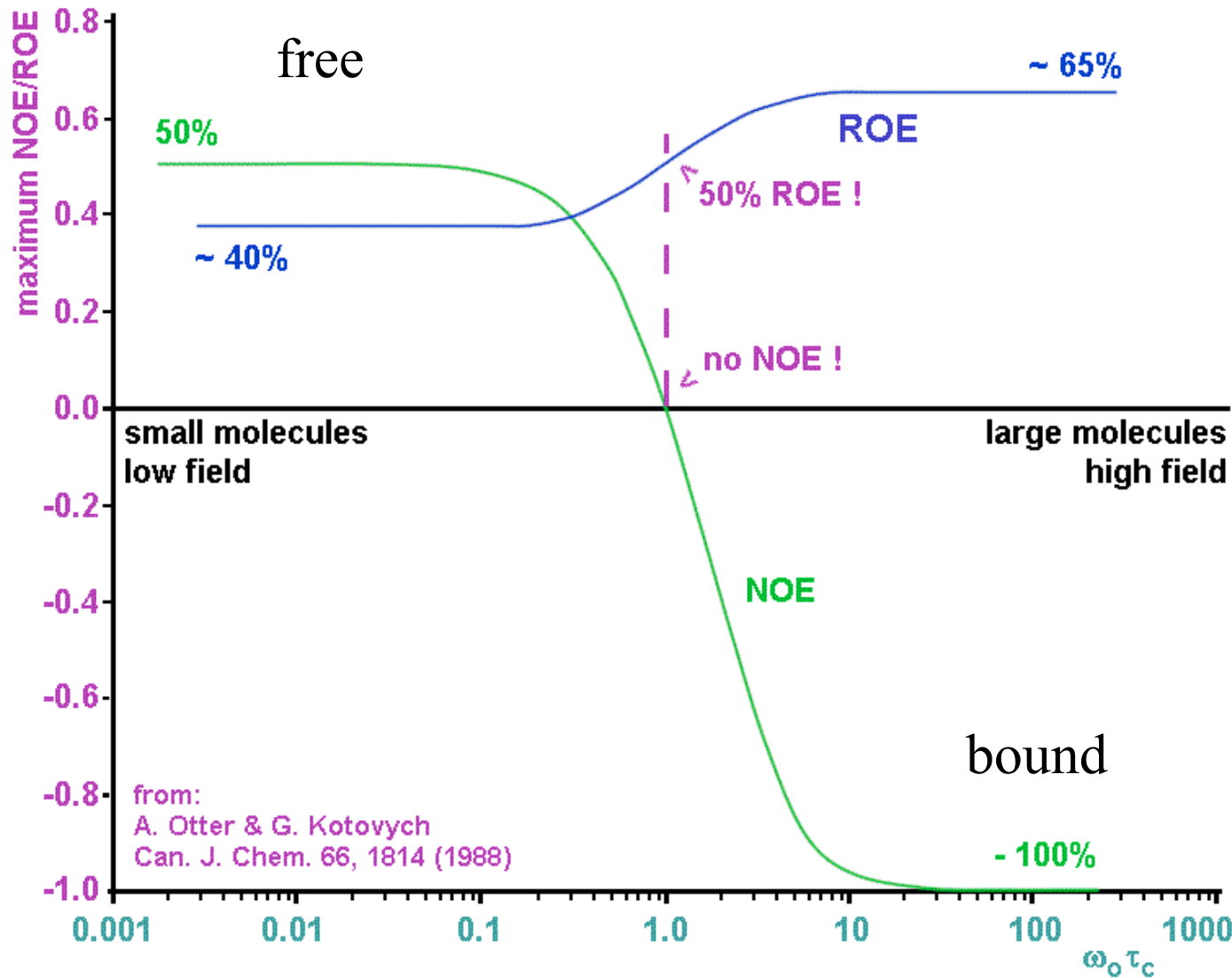
NOE-based Methods

- NOE and Correlation Time (τ_C)
- WaterLOGSY
 - Water-Ligand Observed via Gradient SpectroscopY
- Transferred NOE
- Selective 1D NOE Experiments

Nuclear Overhauser Effect (NOE)s



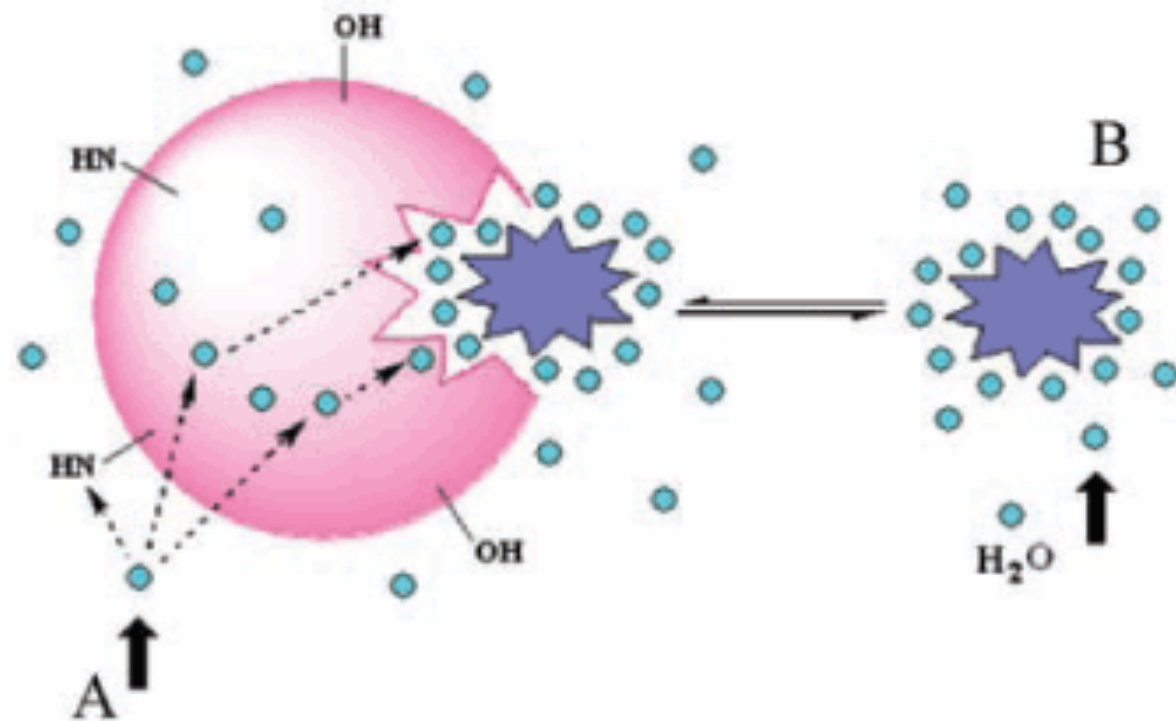
NOE and Correlation Time (τ_c)



Magnetization transfer mechanisms underlying WaterLOGSY. Magnetization transfer from bulk water to ligand occurs via labile receptor protons within and remote from the ligand-binding site as well as from long-lived water molecules within the binding pocket. Dark gray and light gray shading indicate magnetization transfer from inverted water to ligand protons in the slow tumbling (i.e. receptor-ligand complex) and fast tumbling (i.e. free ligand) limits, respectively. Only the hits experience both types of magnetization transfer. The pool of free ligands having experienced inversion transfer from bulk water builds up as ligand continues to exchange on and off the receptor.

WaterLOGSY

*Water-Ligand Observed via Gradient SpectroscopY



Dalvit, C., P. Pevarello, M. Tato, M. Veronesi, A. Vulpetti and M. Sundstrom (2000). "Identification of compounds with binding affinity to proteins via magnetization transfer from bulk water." *Journal of Biomolecular Nmr* **18**(1): 65-68.

Comparison of waterLOGSY versus STD approaches for identifying binders of RNA. Sample and experimental conditions are 0.77 mM ligands, 38 μM RNA (P456, a 52 kDa ribozyme subdomain of 160 nucleotides), 23% H₂O at 278 K and 18.8 T. Top trace, A: reference 1D spectrum of the ligand mixture. Middle trace, B: waterLOGSY results using selective water inversion. Resonances of negative sign are labile ligand protons. Bottom trace, C: STD with selective saturation for 3 s on 5.5 ppm; the total experiment time is the same as that for part B. Only the most intense ligand peaks (7.1-7.2 ppm) are barely distinguishable from noise.

WaterLOGSY Example

Nucleotide Mixture

A

1D Proton

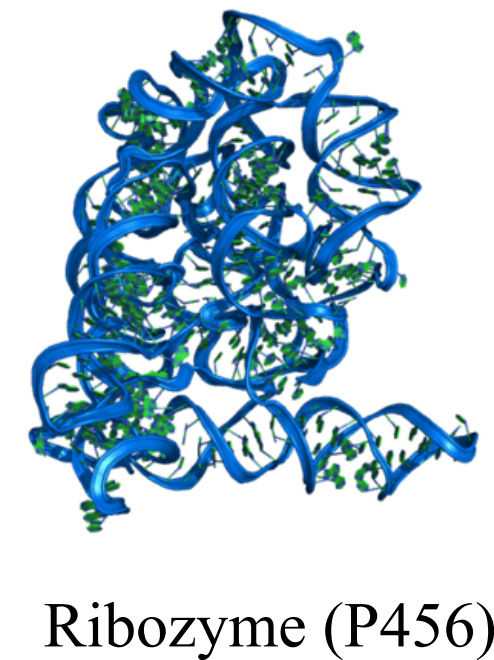
B

WaterLOGSY

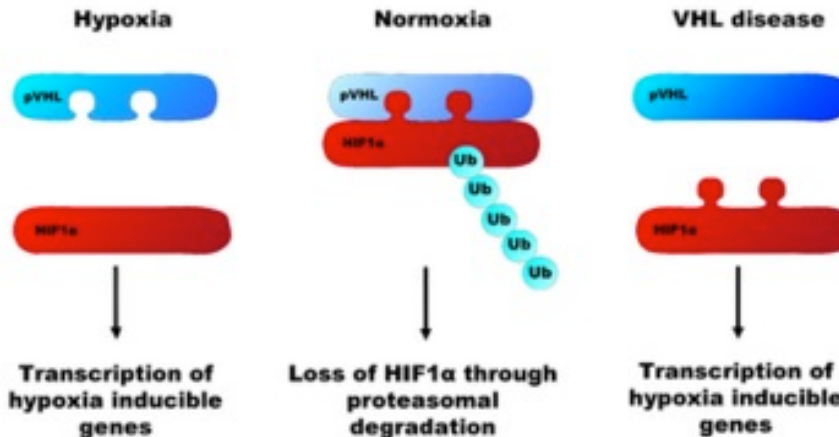
C

STD

9.5 9.0 8.5 8.0 7.5 7.0 6.5 6.0 5.5 5.0 4.5
ppm

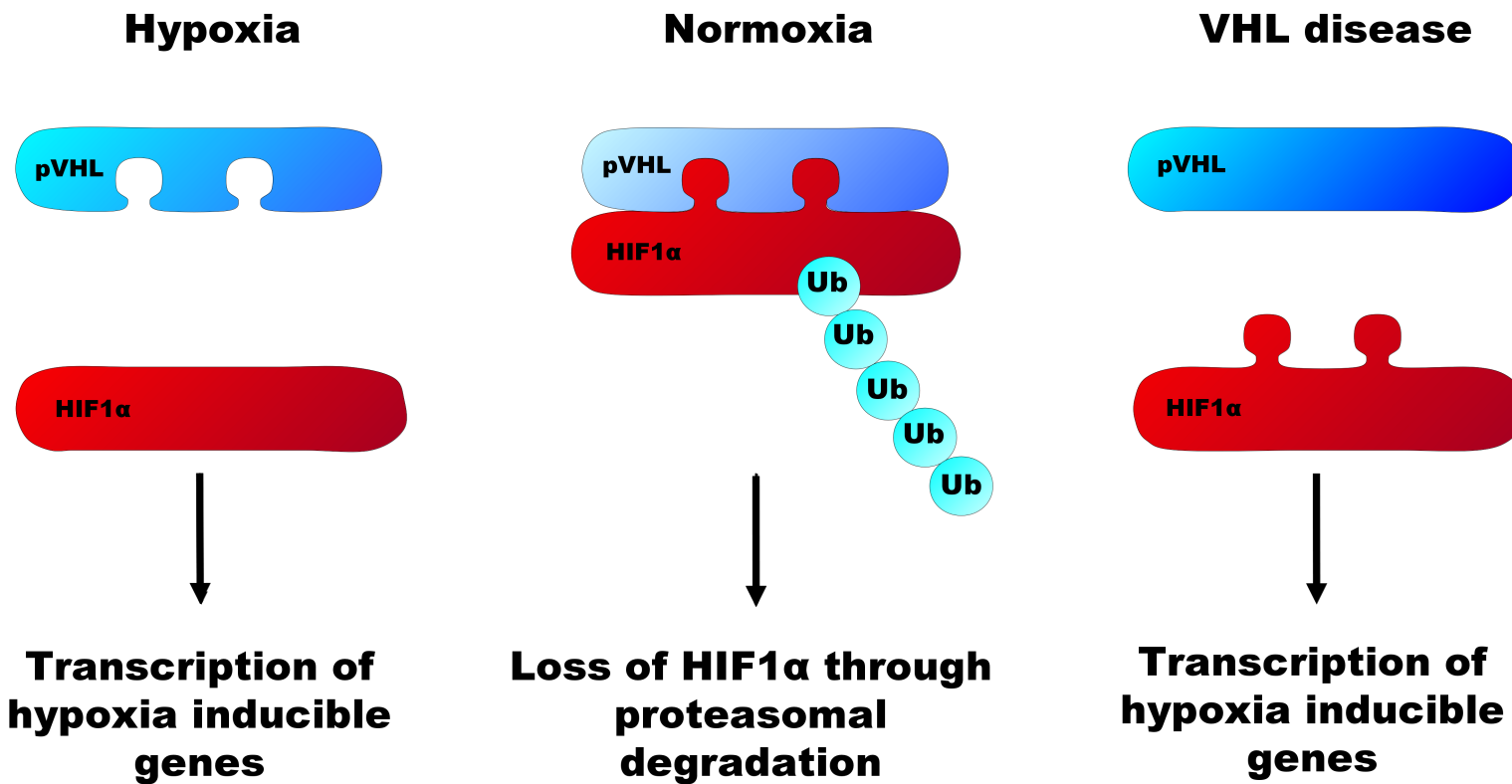


Von Hippel–Lindau disease is inherited in an **autosomal dominant** pattern.



The regulation of HIF1α by pVHL. Under normal oxygen levels, HIF1α binds pVHL through 2 hydroxylated proline residues and is polyubiquitinated by pVHL. This leads to its degradation via the proteasome. During hypoxia, the proline residues are not hydroxylated and pVHL cannot bind. HIF1α causes the transcription of genes that contain the hypoxia response element. In VHL disease, genetic mutations cause alterations to the pVHL protein, usually to the HIF1α binding site.

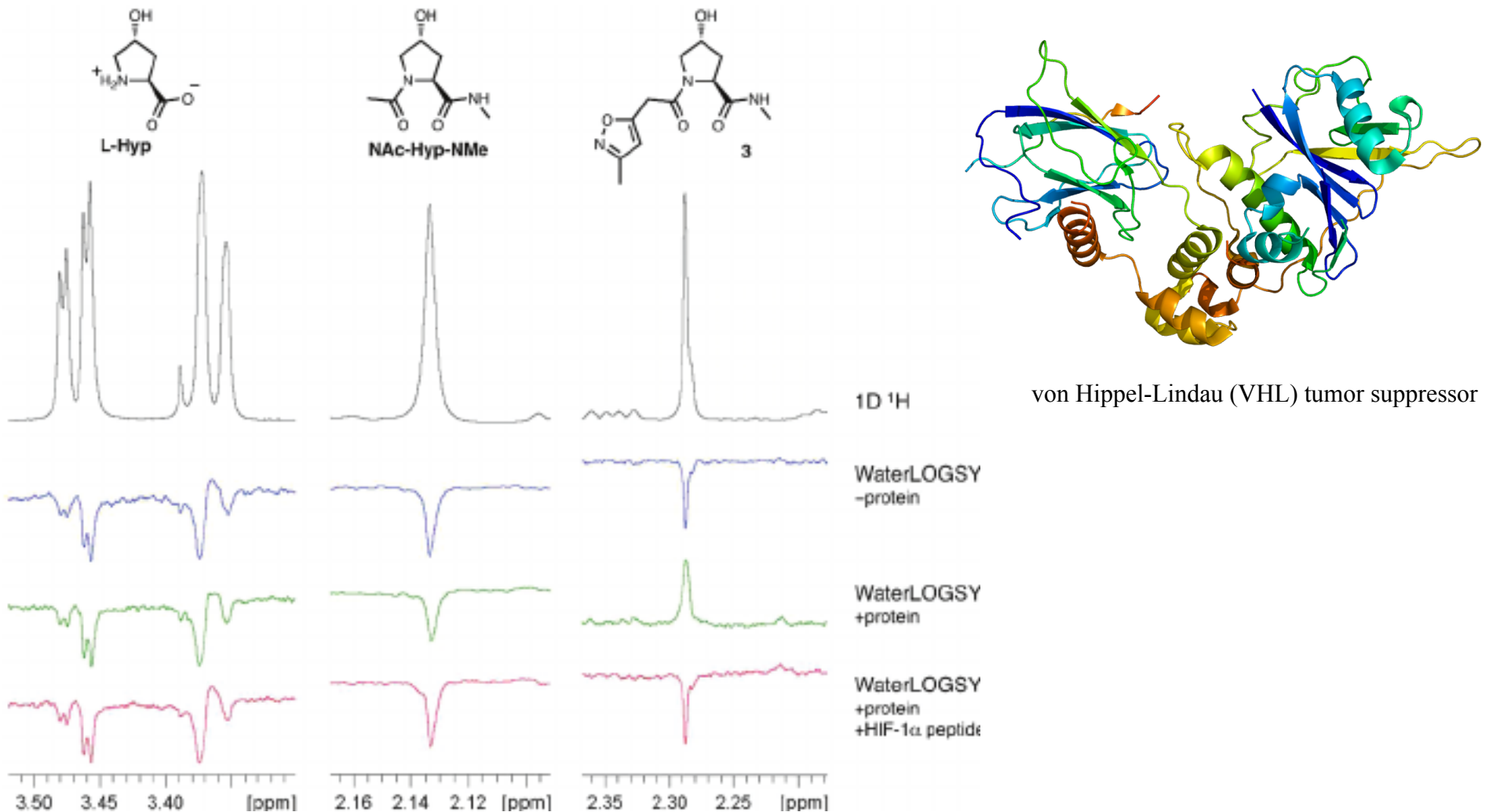
von Hippel-Lindau (pVHL) tumor suppressor



HIF= hypoxia-inducible factor 1 alpha

Figure 2. WaterLOGSY NMR spectroscopy shows binding of 3, but not L-Hyp or NAc-Hyp-NMe, to VHL.

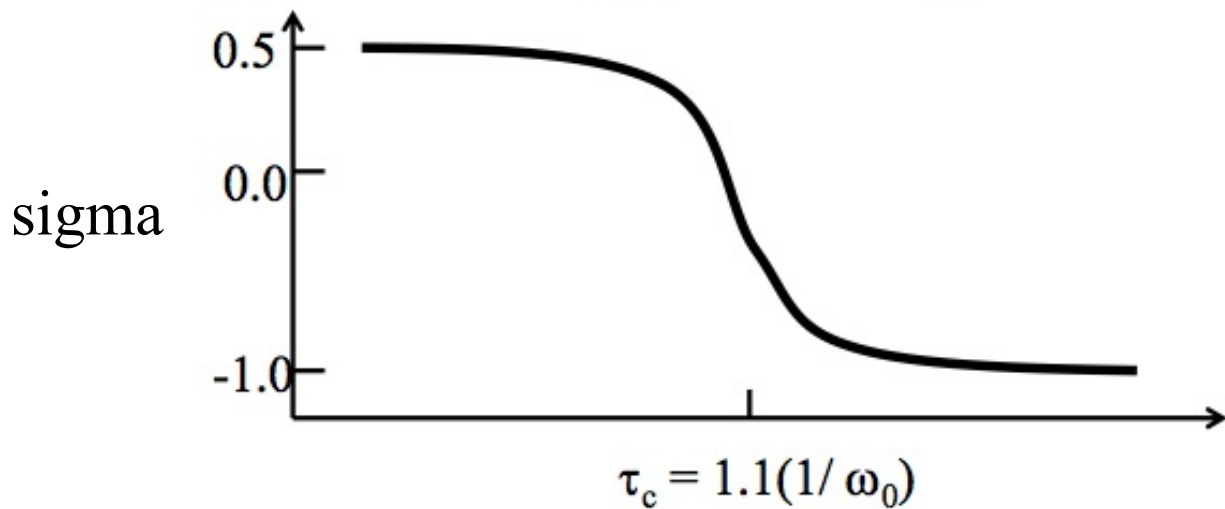
WaterLOGSY Example



Buckley et al., Targeting the von Hippel-Lindau E3 Ubiquitin Ligase Using Small Molecules to Disrupt the VHL/HIF-1 α . J. Am. Chem. Soc. 2012, 134(10), pp. 4465-4468.

Transferred NOE

NOEs from large and small molecules
have opposite signs



Rates of transfer (σ) are proportional to τ_c for large molecules.

Observe: $\text{NOE}(\text{obs}) = p(\text{bound}) \cdot \sigma(\text{bound}) + p(\text{free}) \cdot \sigma(\text{free})$

NOE from bound state dominates for $p(\text{bound})/p(\text{free}) > 0.05$

The transfer NOE can be used to screen for small molecules that bind to a receptor **under conditions of fast exchange**. No isotopic labeling of the ligand or receptor is necessary. Even under conditions where there is only a small percentage of bound ligand in solution, the “memory” of NOEs present within the bound state conformation of the ligand are carried over to the ligand free in solution under conditions of *fast exchange* and nOEs will appear if binding occurs:

Transferred NOE

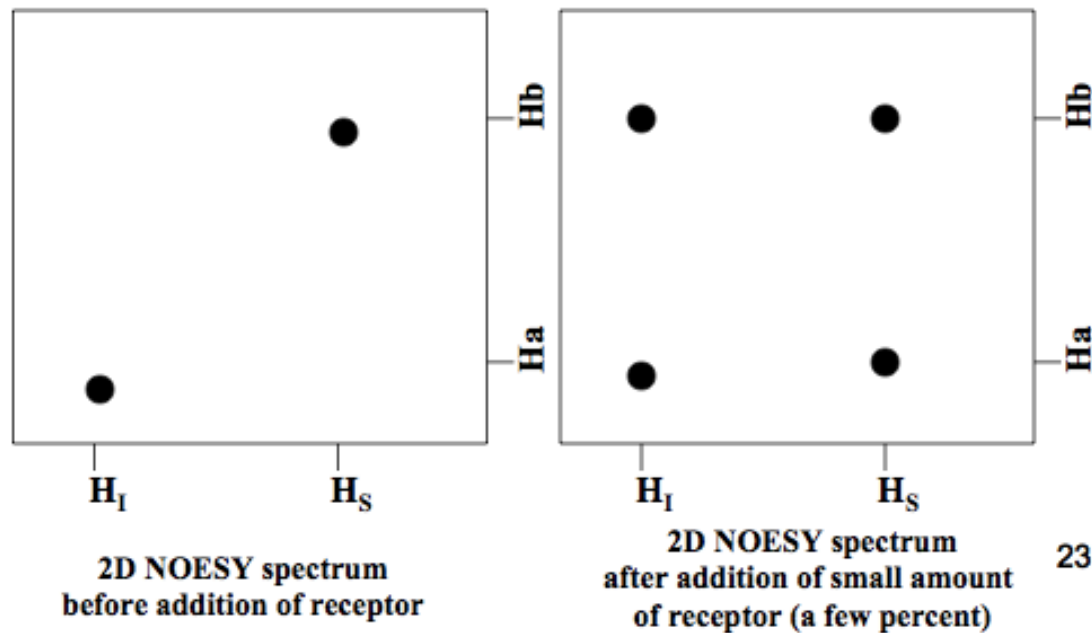
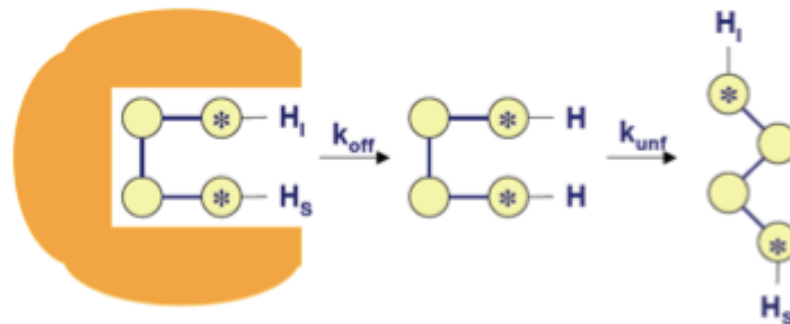
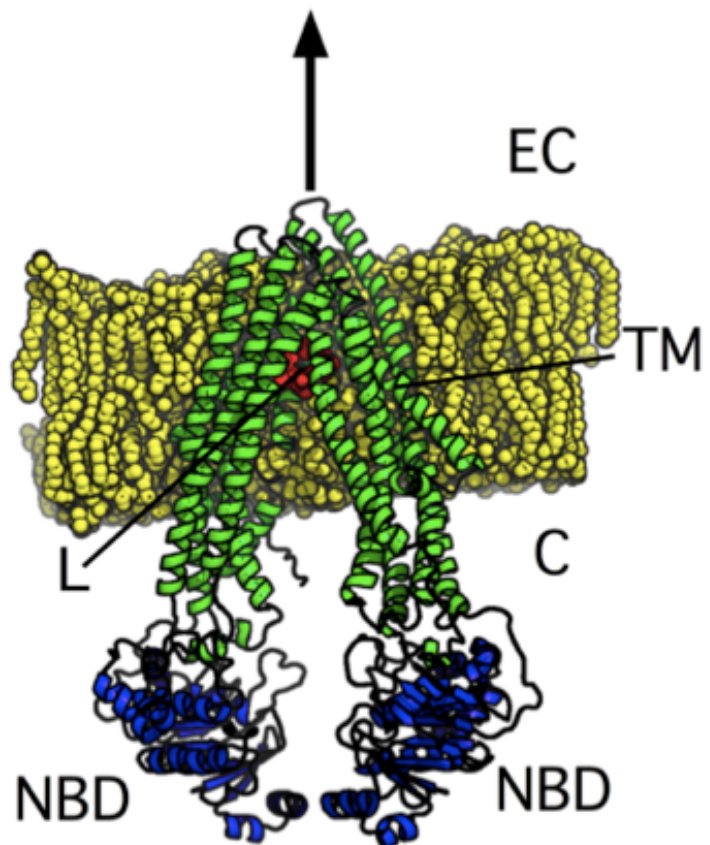
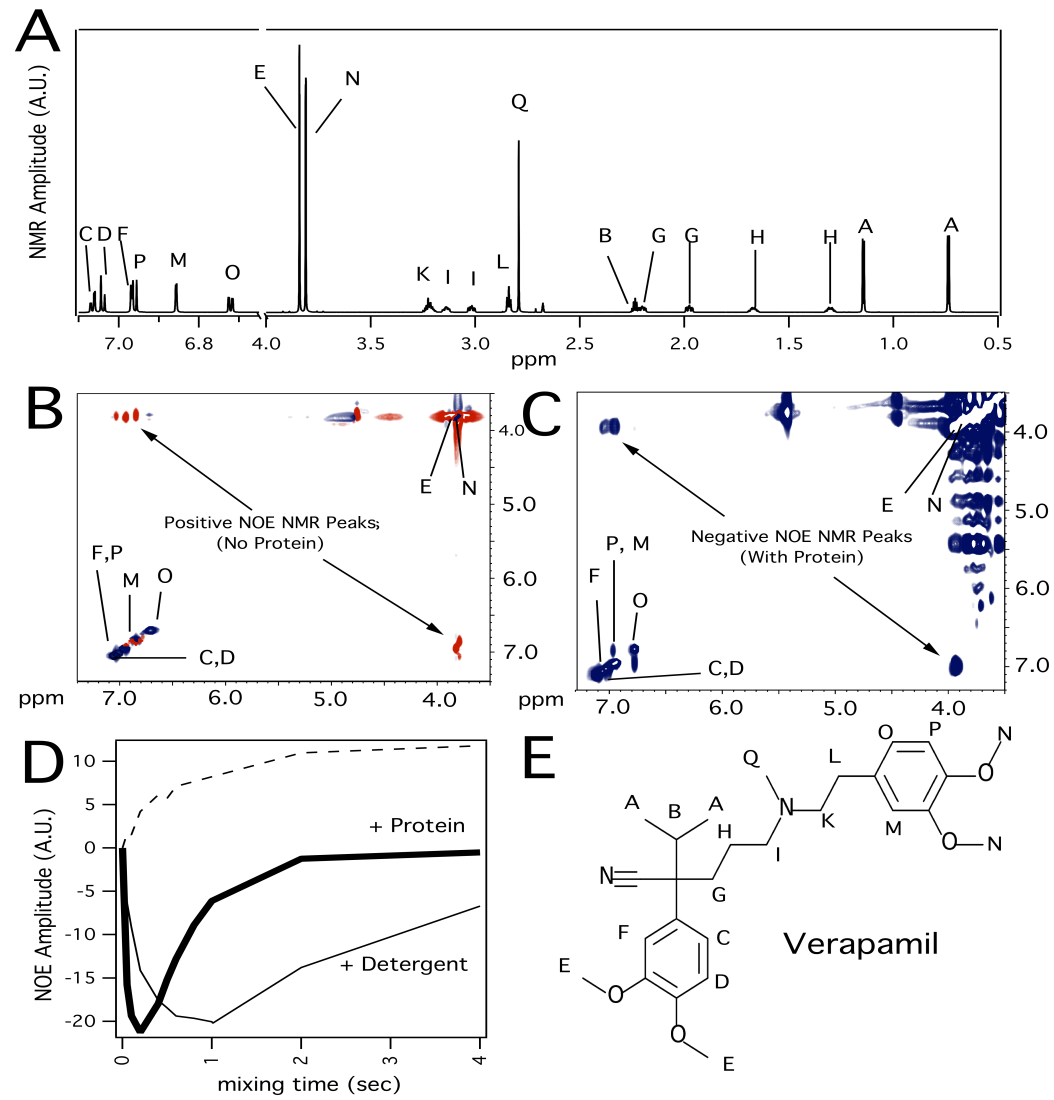
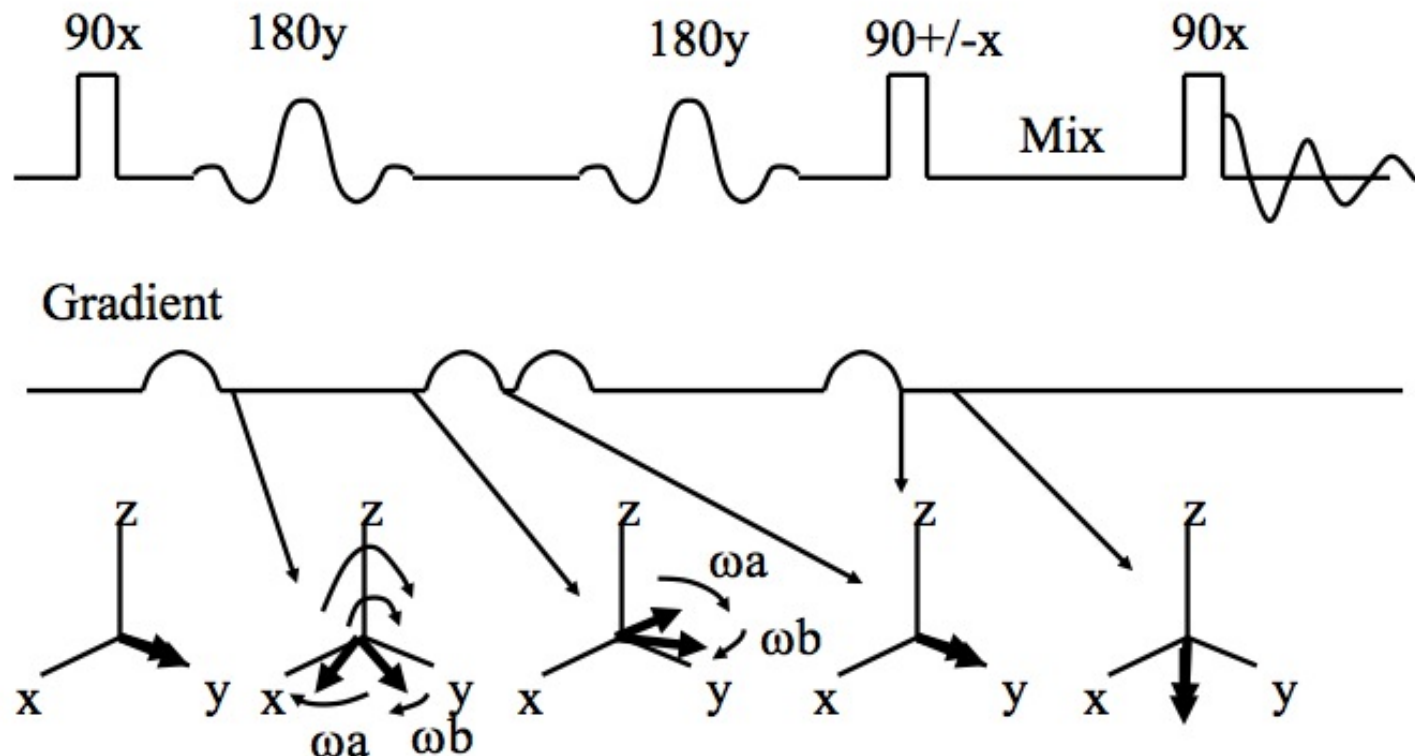


Figure 7. 1D proton and et-NOE spectroscopy of 4 mM verapamil in the presence and absence of 40 μ M mouse MDR3 transporter solubilized in 0.1% DM. A) 1D proton NMR spectrum of 4 mM verapamil with NMR peak assignments. 2D NOE spectra of B) 4 mM verapamil without protein and a mixing time of 800 ms and C) 4 mM verapamil with 40 μ M protein and a mixing time of 150 ms. D) NOE buildup between protons M and N with 40 μ M protein (thick line), with 0.1% DM (thin line) and without detergent and protein (dotted line). E) The labeled molecular structure of verapamil.

Transferred NOE Example

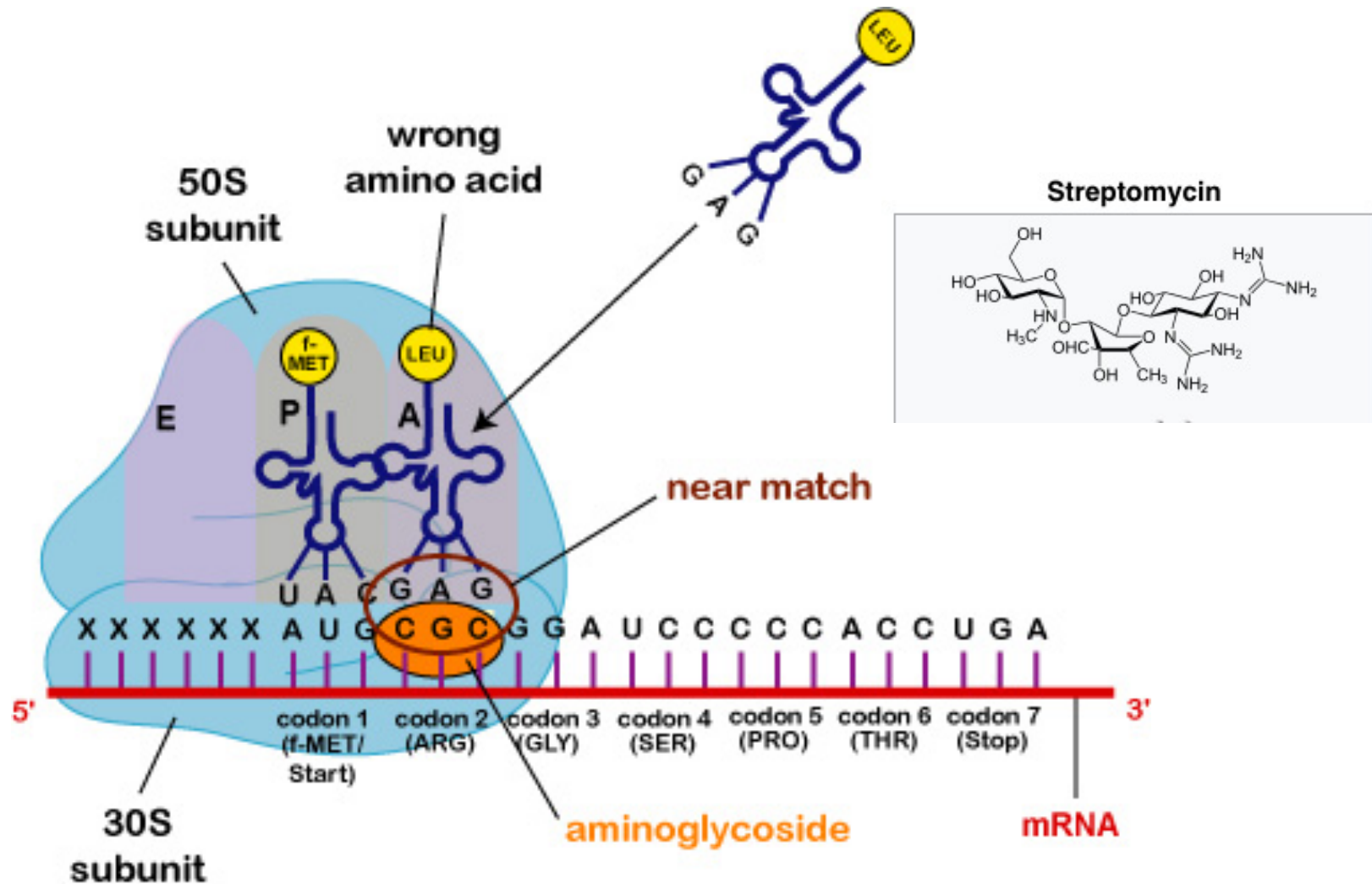


Selective 1D NOE



Behavior for selected resonance from two different volume elements on $+x$ 90° pulse. Vectors return to $+z$ with $-x$ 90° pulse.

Anti-biotics: Aminoglycosides



Improving Aminoglycosides

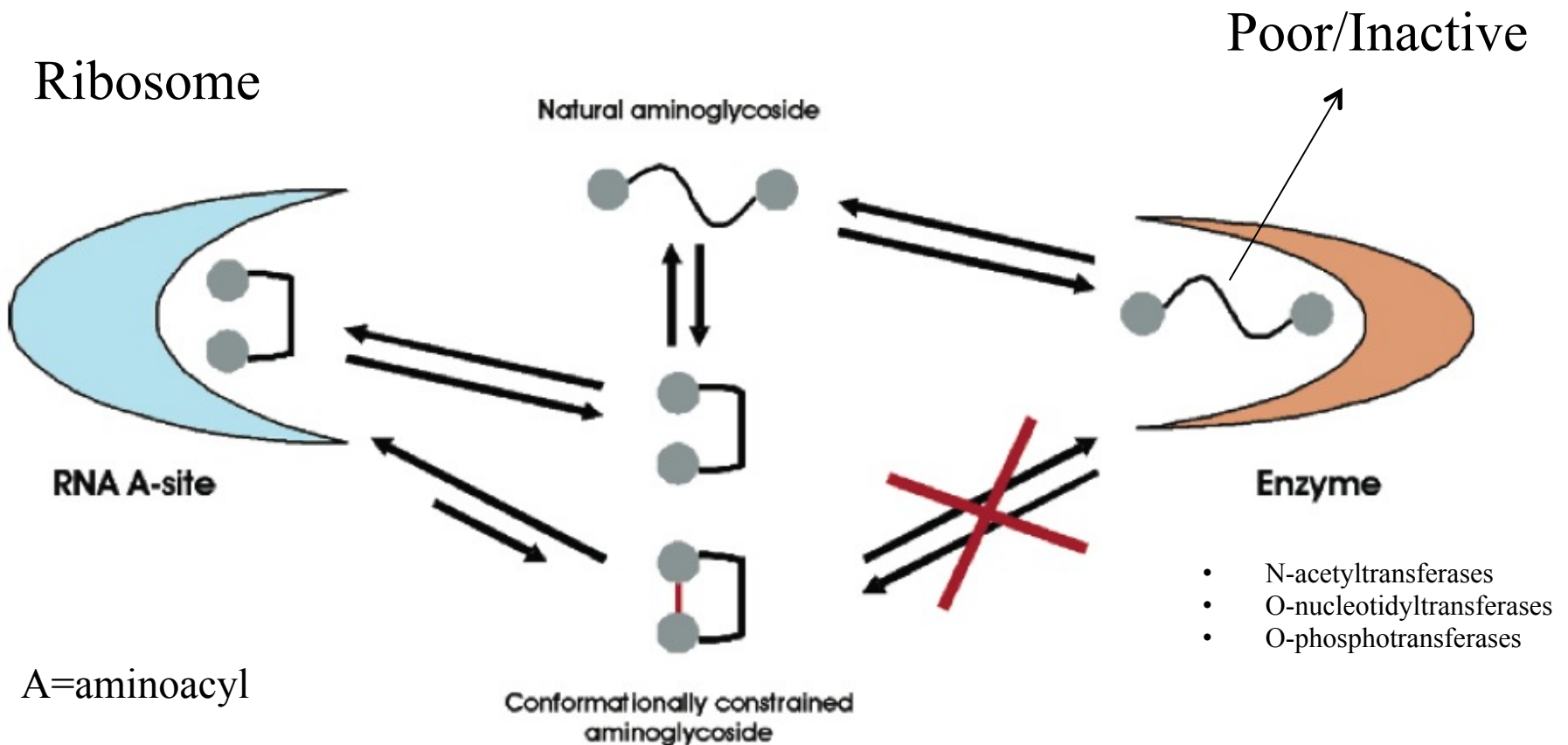
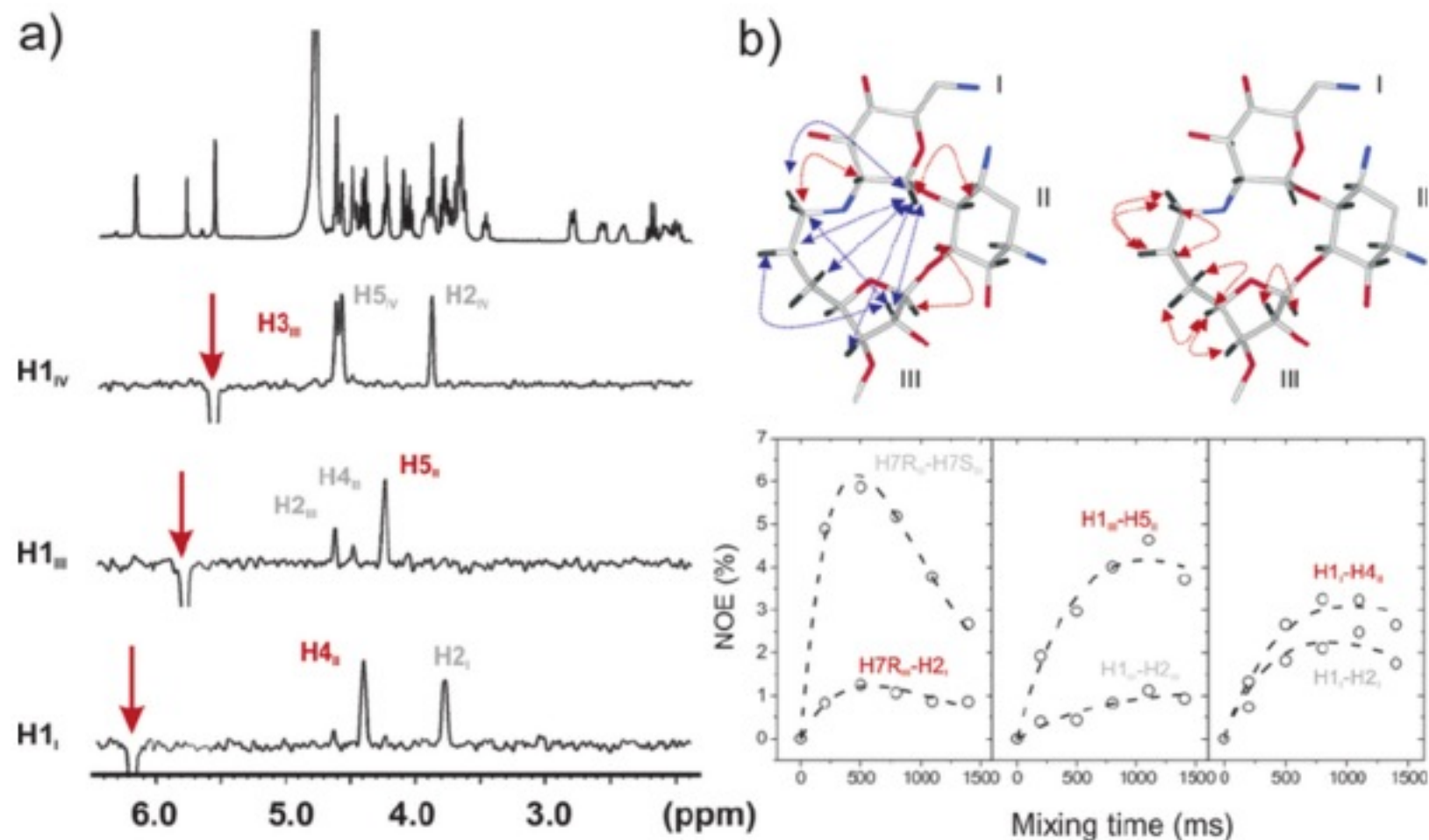
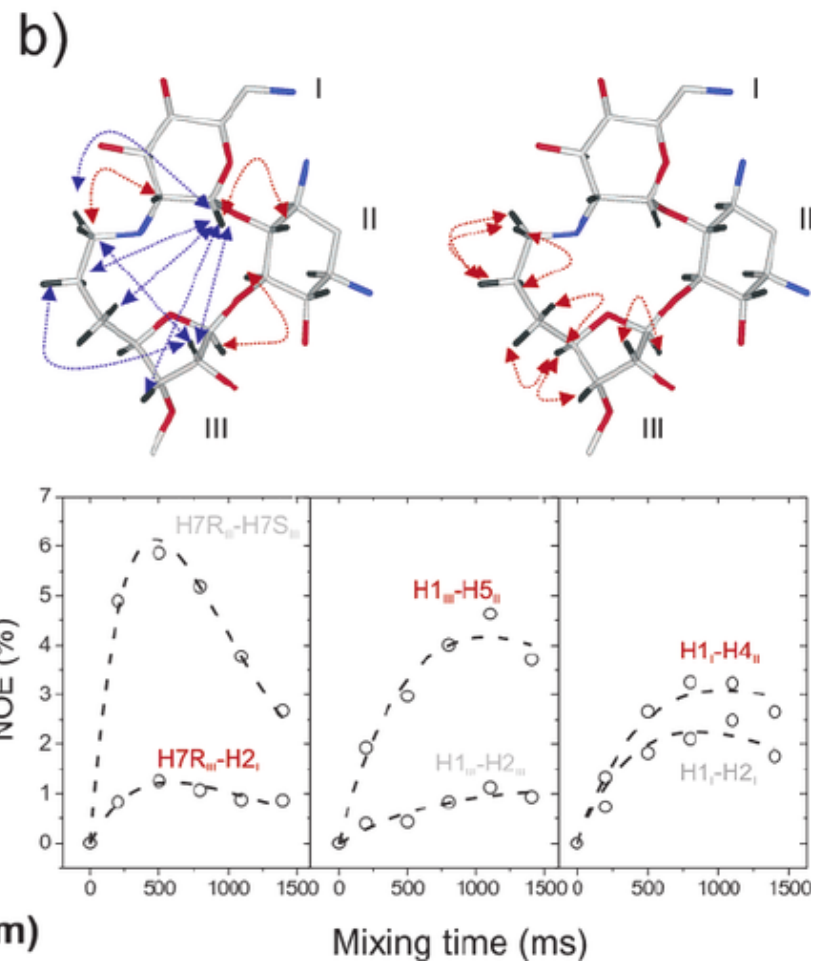
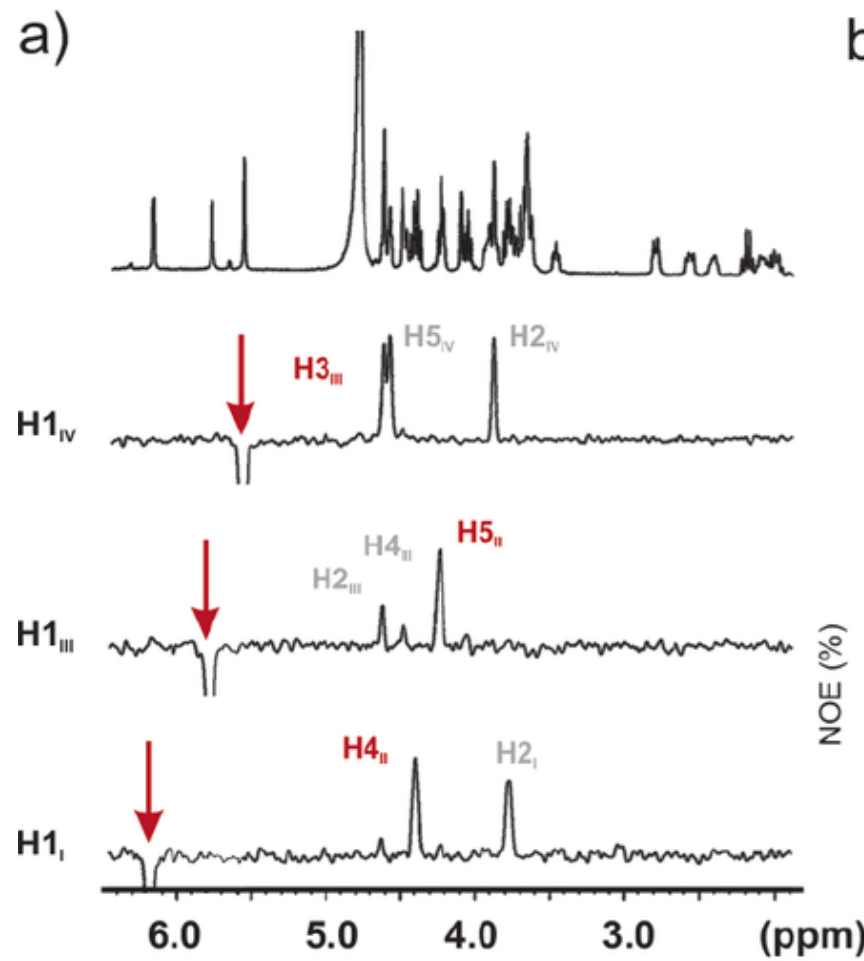


Figure 2. (a) Selective 1D NOE experiments with the 1D-DPFGSE NOE pulse sequence, corresponding to the inversion of the anomeric protons in compound 3. (b) Upper panel: Schematic representation of some of the experimental information employed in the structural analysis of 3. The upper left panel shows the observed NOEs as red arrows and those not observed as blue arrows. The upper right panel shows the structurally relevant experimental J couplings measured for 3. The ring IV is omitted for simplicity. Lower panel: some representative NOE buildup curves. NOEs corresponding to known fixed distances, employed as references, are labeled in gray. NOEs corresponding to unknown distances are labeled in red.



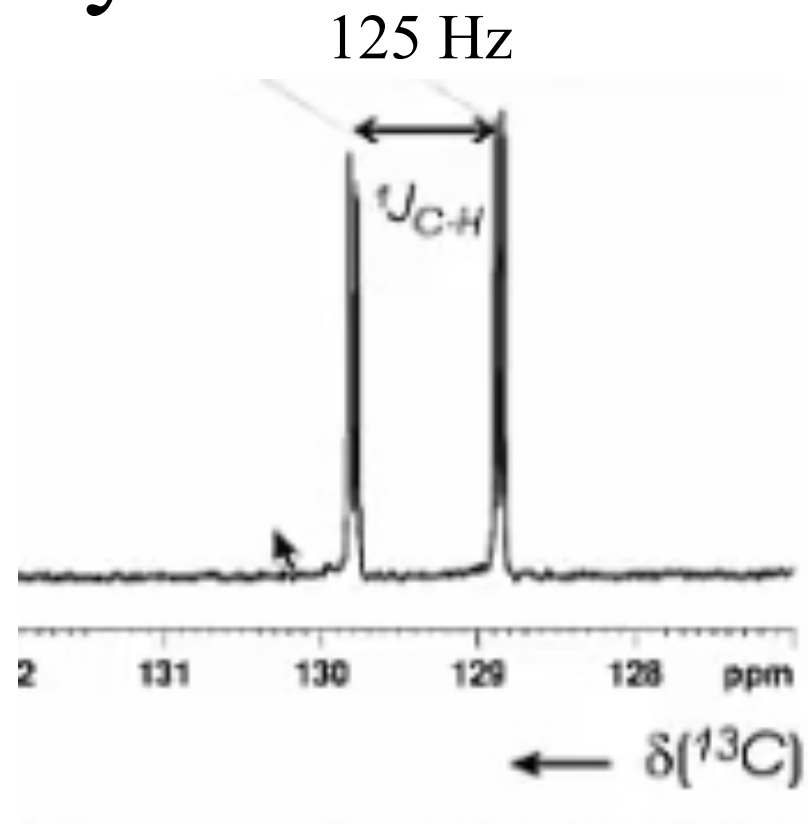
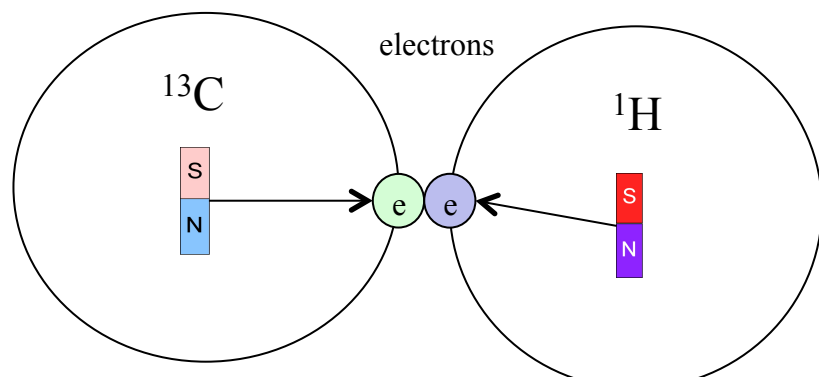
Selective 1D NOE



Ligand-based NMR Screening

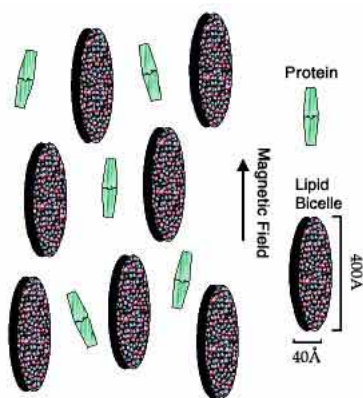
- **Chemical Shift**
- **Saturation Transfer Difference**
- **Relaxation Methods**
- **Diffusion Editing**
- **NOE-based Methods**
- **Residual Dipolar Couplings**
- Other

J-Coupling: Interaction Through a Proxy

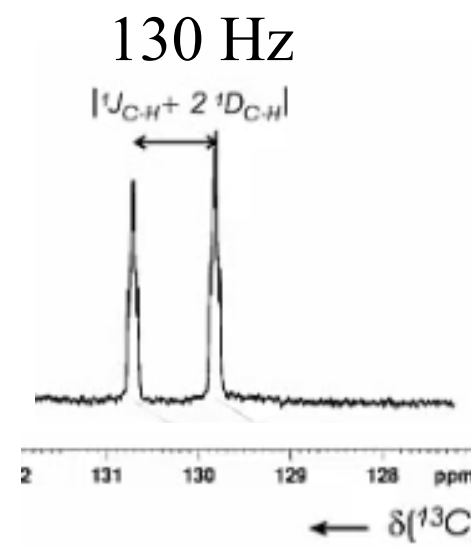
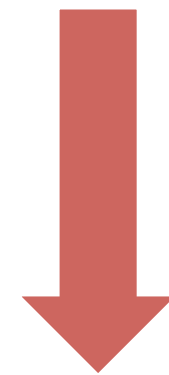
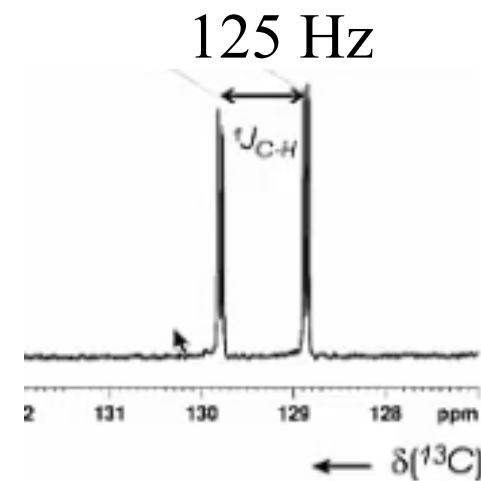
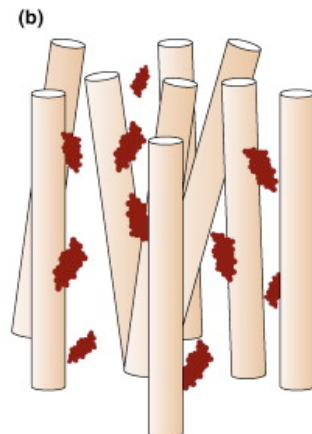


Residual Dipolar Coupling (RDC)

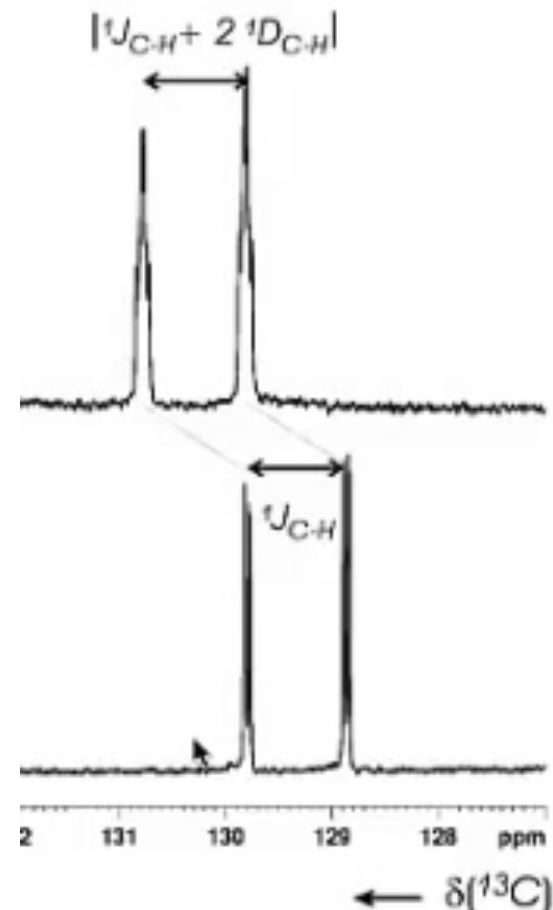
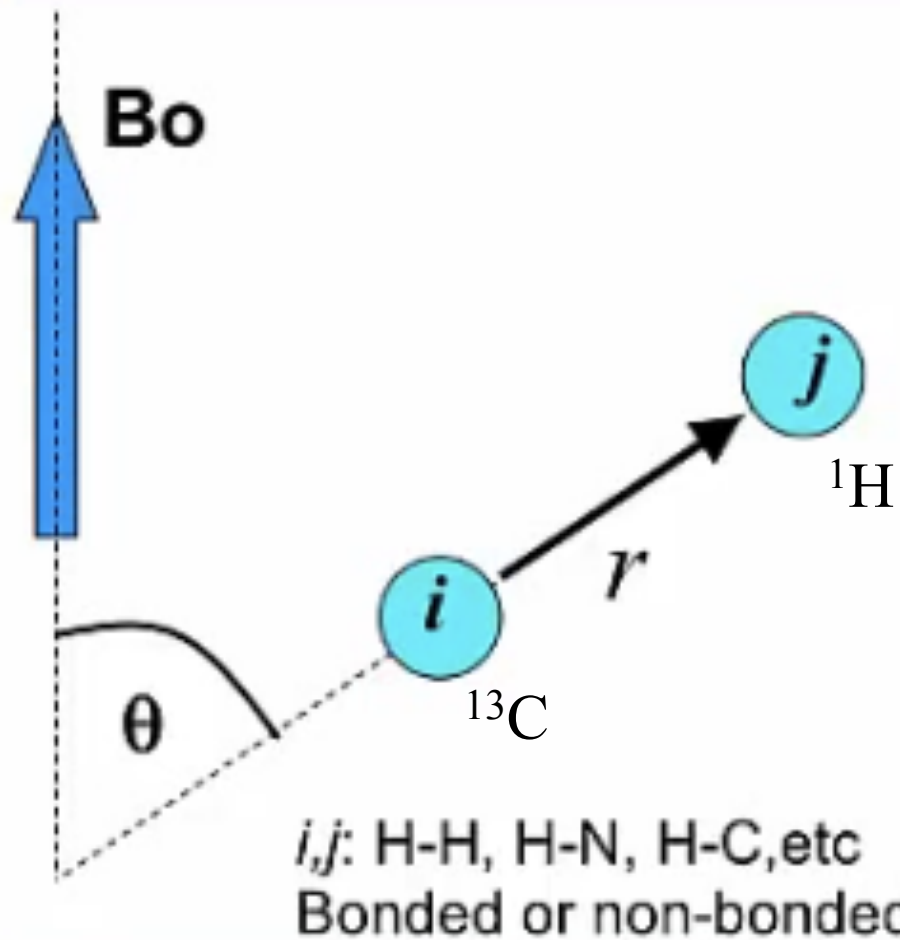
Bicelles



Pf1 Filamentous Phage



Residual Dipolar Coupling (RDC)



$$D_{ij} = \frac{\kappa}{r_{ij}^3} \left(\cos^2 \theta - \frac{1}{3} \right)$$

$$\kappa = -\frac{3}{8\pi^2} \gamma_i \gamma_j \mu_o \hbar$$

The maximum value for $\cos^2 \theta$ is 1
(for $\theta = 0$ or π)

Why RDCs?

- long-range restraint
 - NOEs, J-coupling, all short
- relative orientations

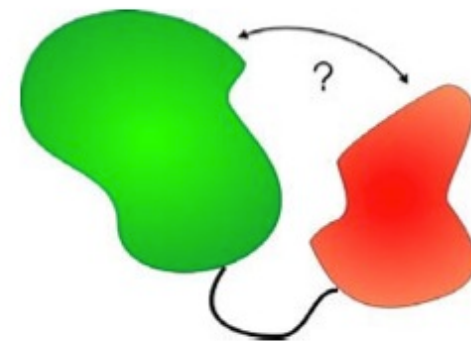
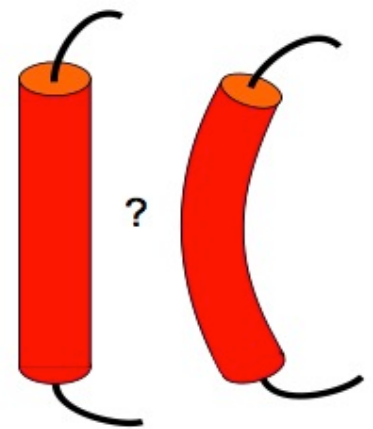
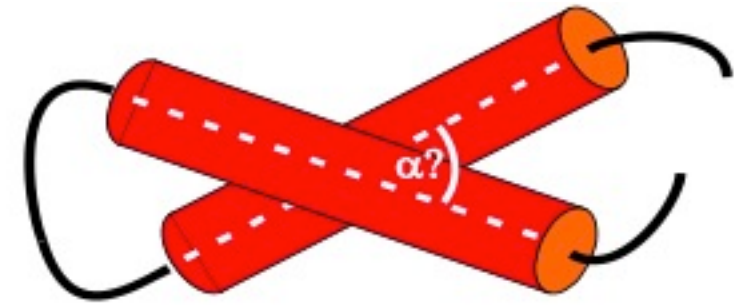
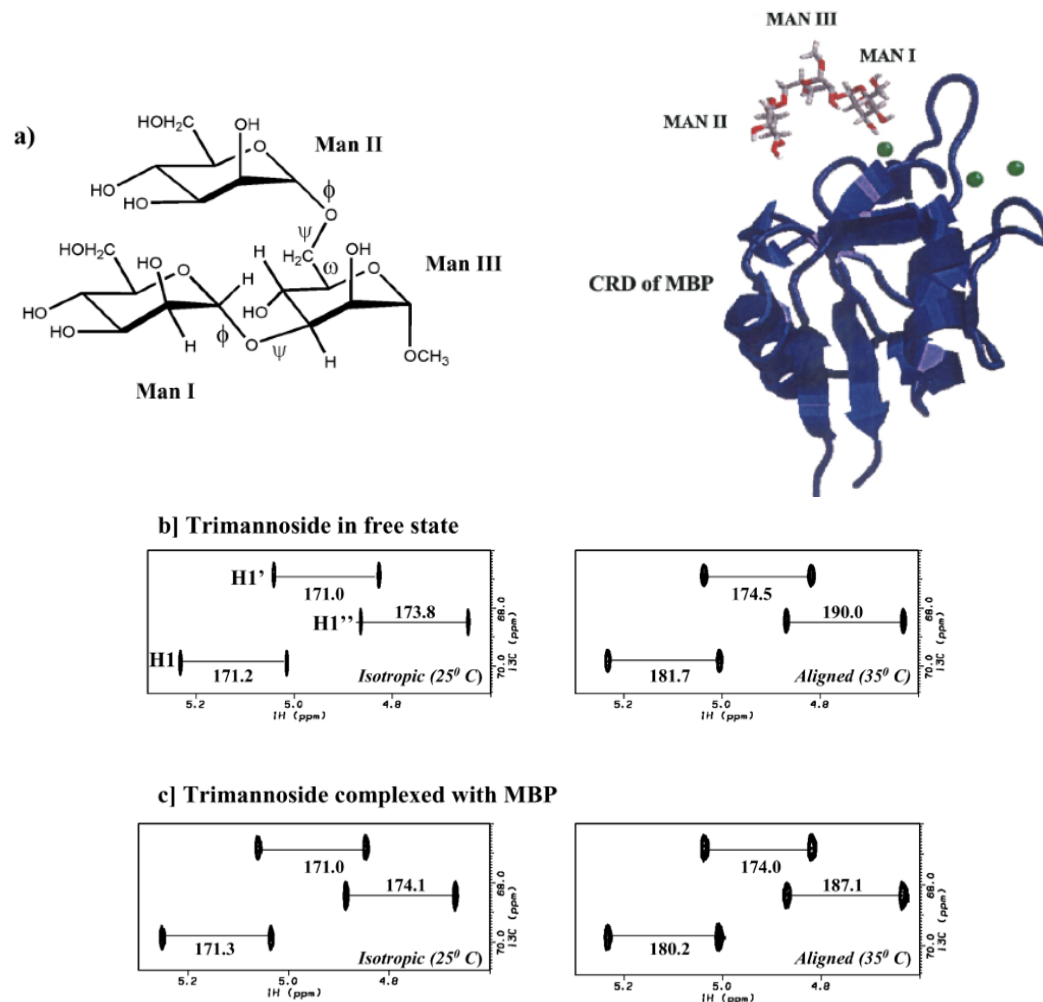
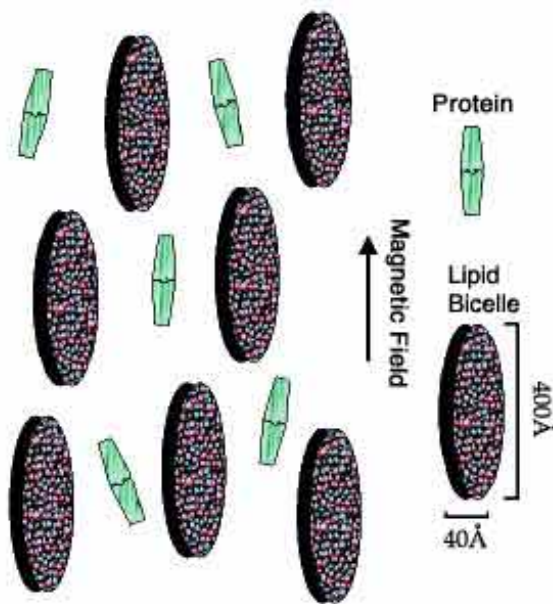


Figure 7. (a) Trimannoside ligand used for binding studies with MBP. Man I, Man II and Man III represent rings 1, 2 and 3 of trimannoside, respectively, while ϕ , ψ , ω represent the glycosidic dihedral angles. (b) Section of a ^1H - ^{13}C coupled HSQC spectra of trimannoside showing ^1H - ^{13}C couplings in the anomeric region of the three mannose units in the free state and (c) in complex with trimeric MBP. Spectra were recorded for the two samples in isotropic phase and in aligned phase (10% (w/v) bicelle solution). RDCs were calculated as the difference between the coupling values in isotropic and aligned phase shown on the spectra.

Residual Dipolar Couplings



Jain, N. U., S. Noble, et al. (2003). "Structural characterization of a mannose-binding protein-trimannoside complex using residual dipolar couplings." *Journal of Molecular Biology* **328**(2): 451-462.

Ligand-based NMR Screening

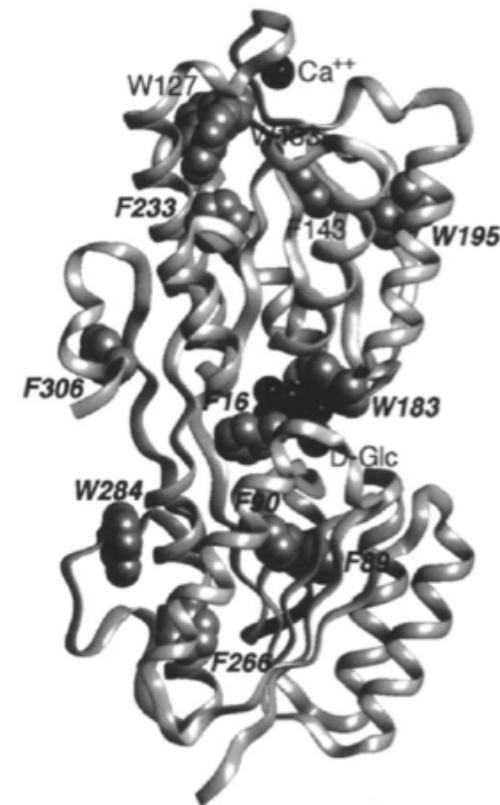
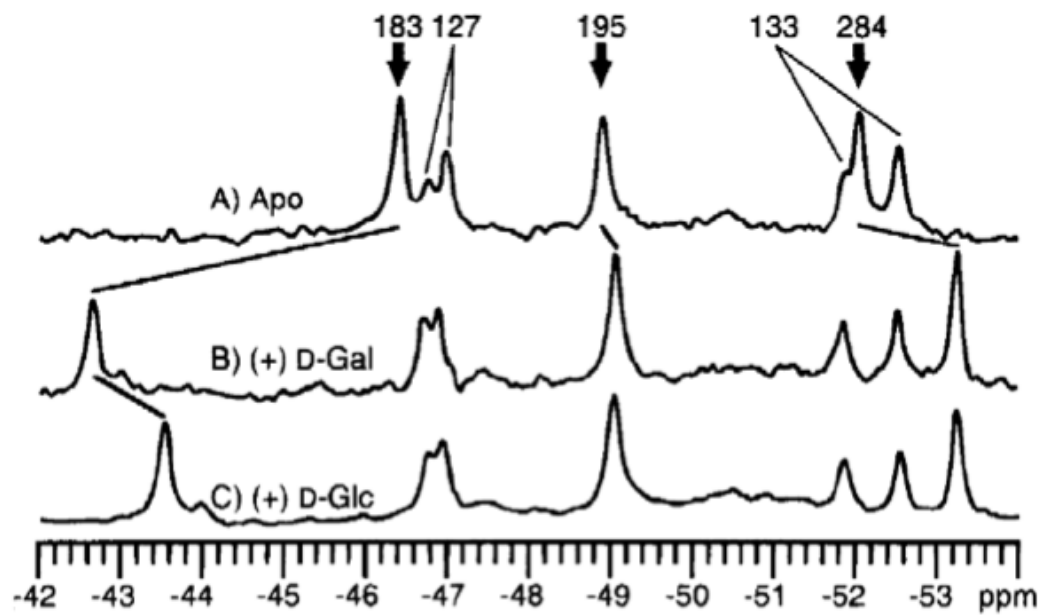
- **Chemical Shift**
- **Saturation Transfer Difference**
- **Relaxation Methods**
- **Diffusion Editing**
- **NOE-based Methods**
- **Residual Dipolar Couplings**
- **Other**

Other Methods of Ligand Based Screening

- **^{19}F -Labeling**
- Paramagnetic Relaxation Enhancement (PRE) NMR
- Pseudo Contact Shift (PCS) NMR

Effect of D-galactose and D-glucose on the ^{19}F NMR spectrum of the 5-F Trp labeled galactose-binding protein (470 MHz) (54). (A) The spectrum of the sugar empty protein. (B) The protein saturated with D-galactose. (C) The protein saturated with D-glucose. (***bold arrows***) Resonances for which significant ligand induced chemical shift changes are observed. The greatest changes are observed for the resonance from the Trp183 position, which lies in van der Waals contact with the bound sugar molecule.

Other: ^{19}F -labeling

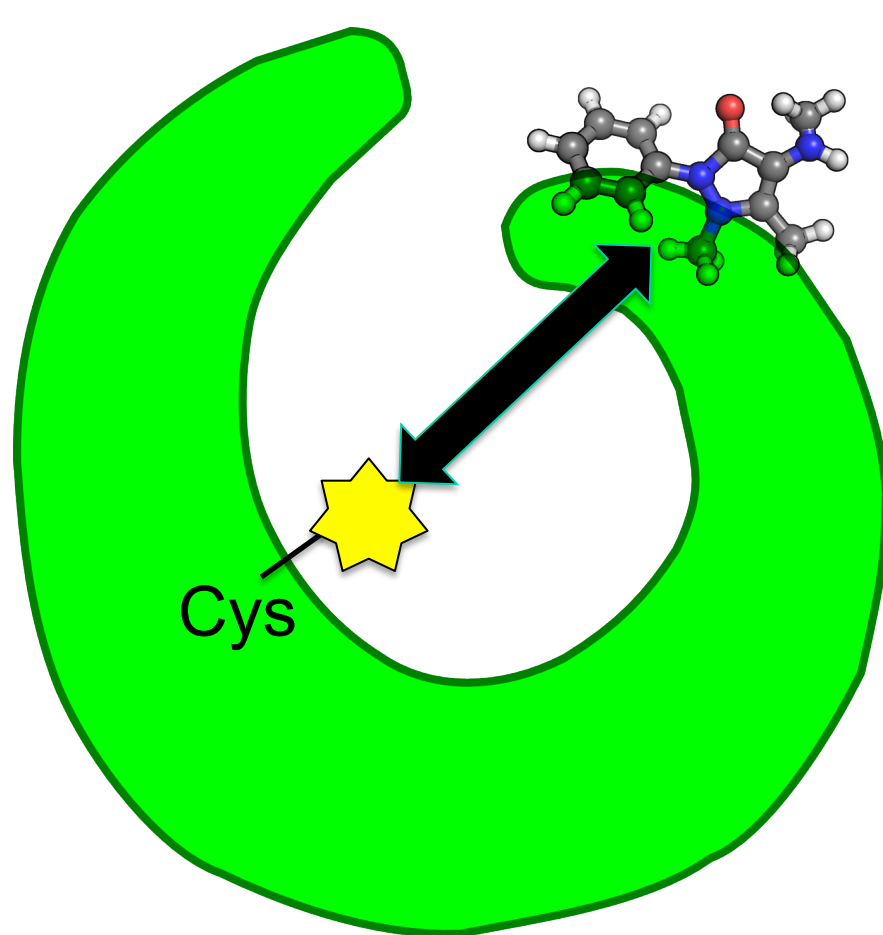


Galactose
Binding
Protein

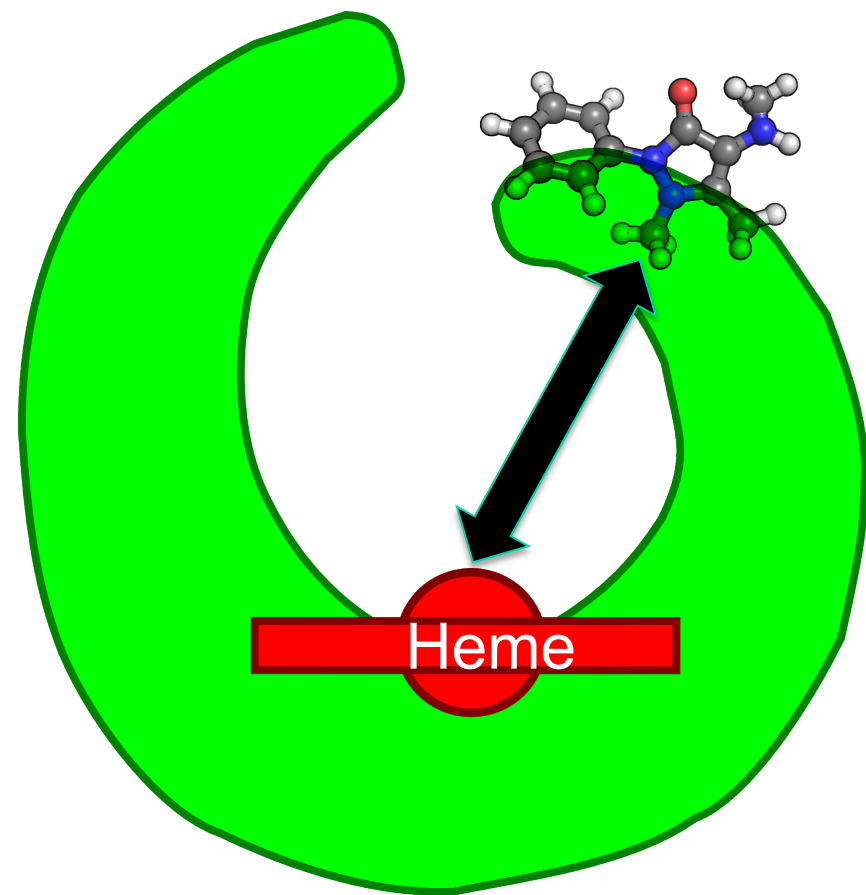
Other Methods of Ligand Based Screening

- **^{19}F -Labeling**
- **Paramagnetic Relaxation Enhancement (PRE) NMR**
- Pseudo Contact Shift (PCS) NMR

Position/Orientation: Paramagnetic Relaxation Enhancement (PRE) NMR

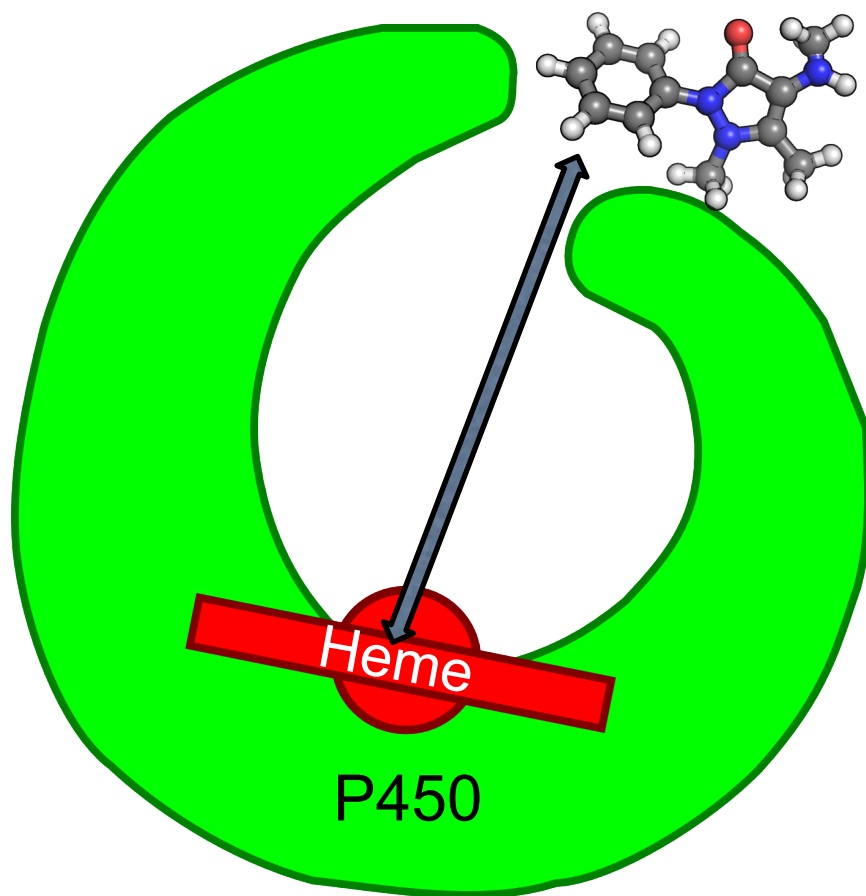


Paramagnetically-Labeled Residue

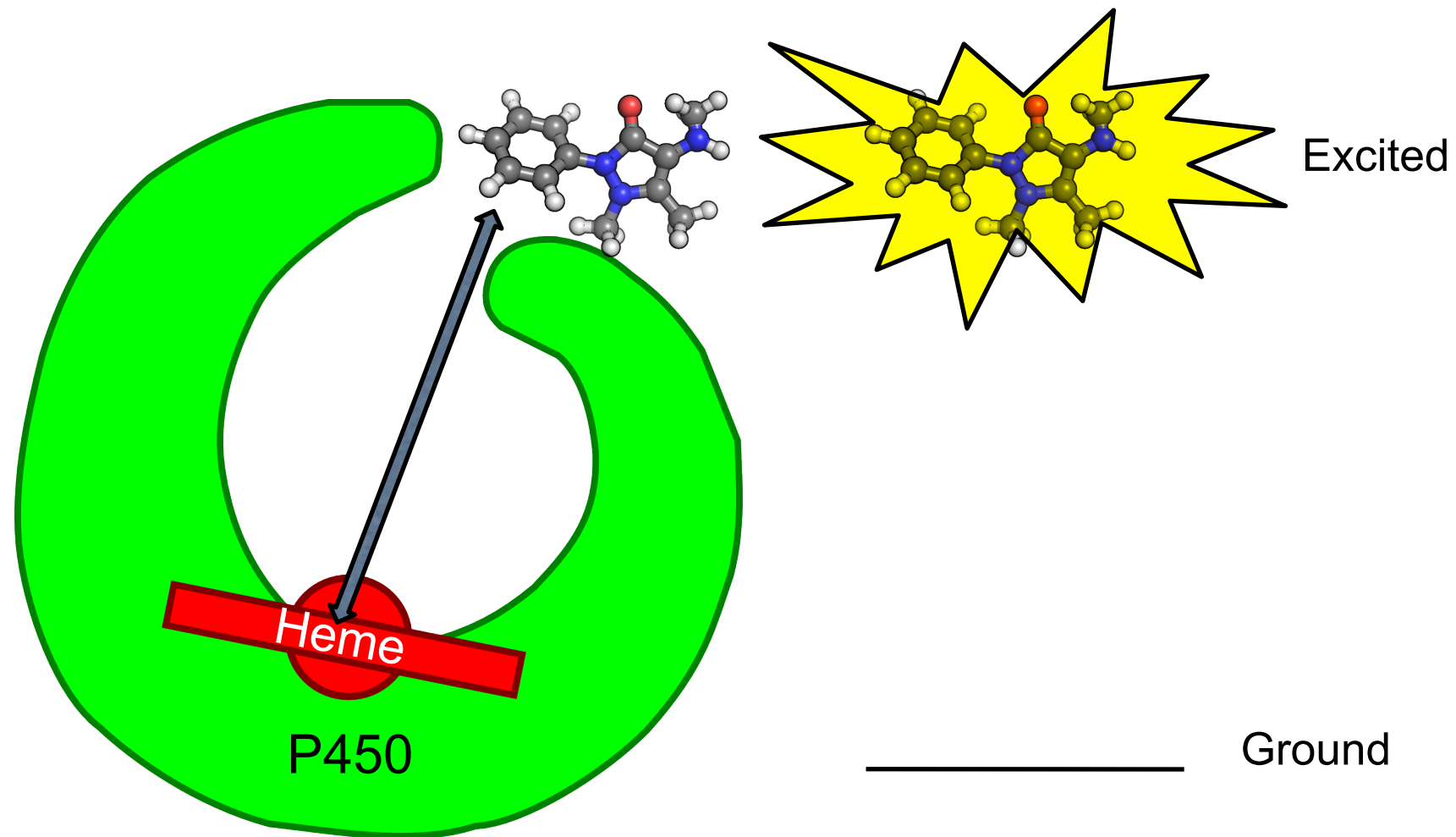


Intrinsic Paramagnetic Label

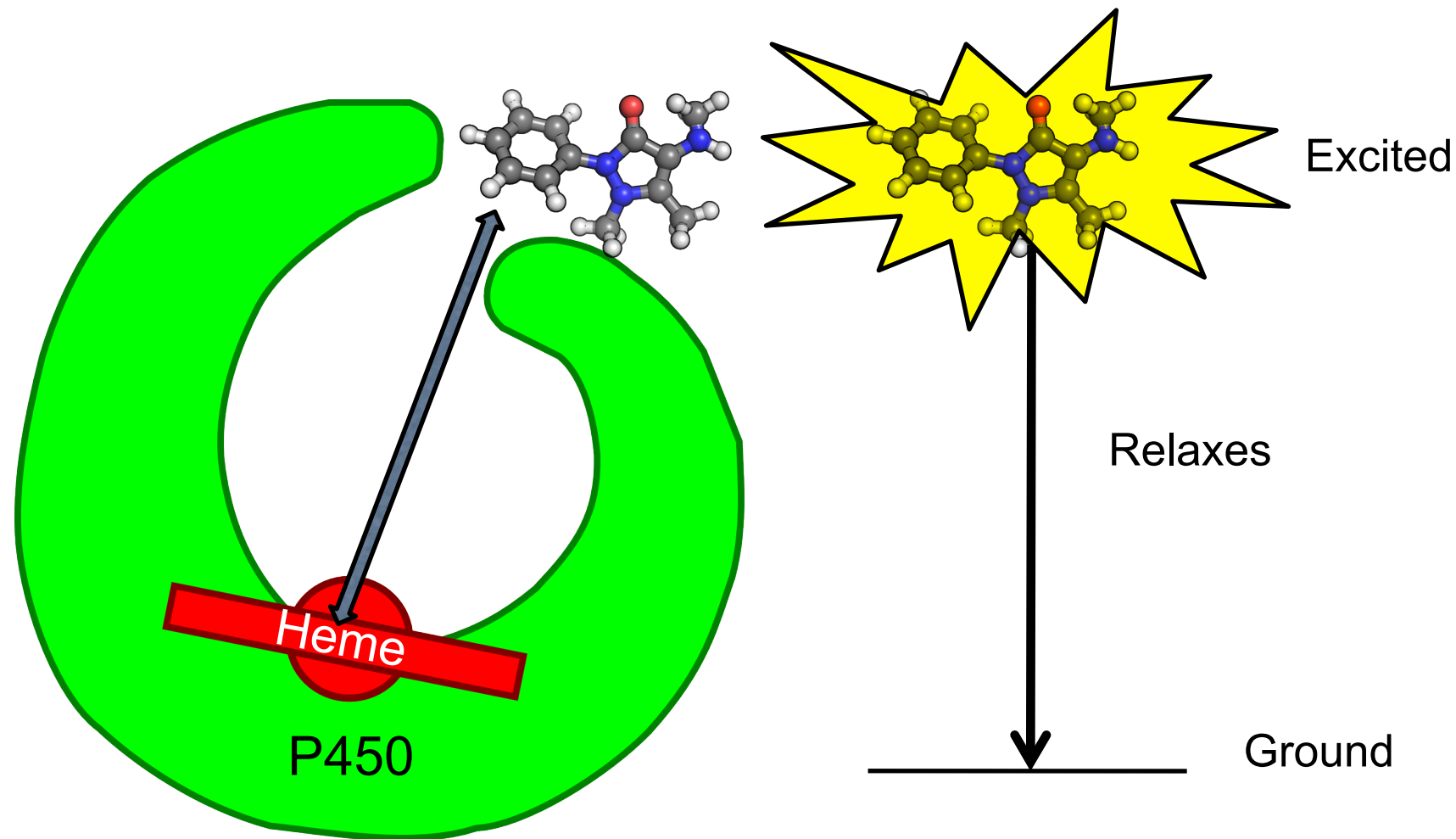
Position/Orientation: PRE NMR



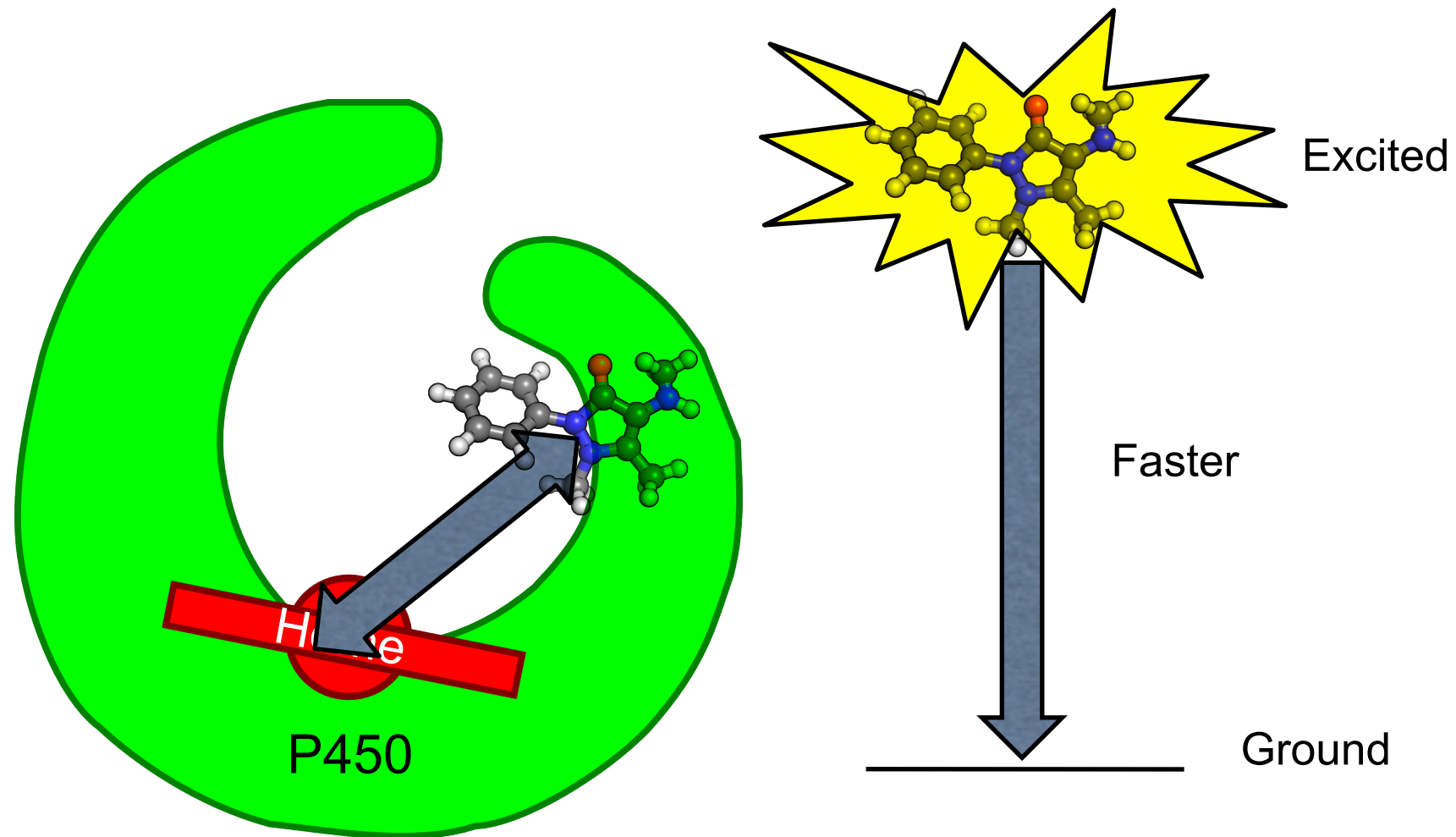
Position/Orientation: PRE NMR



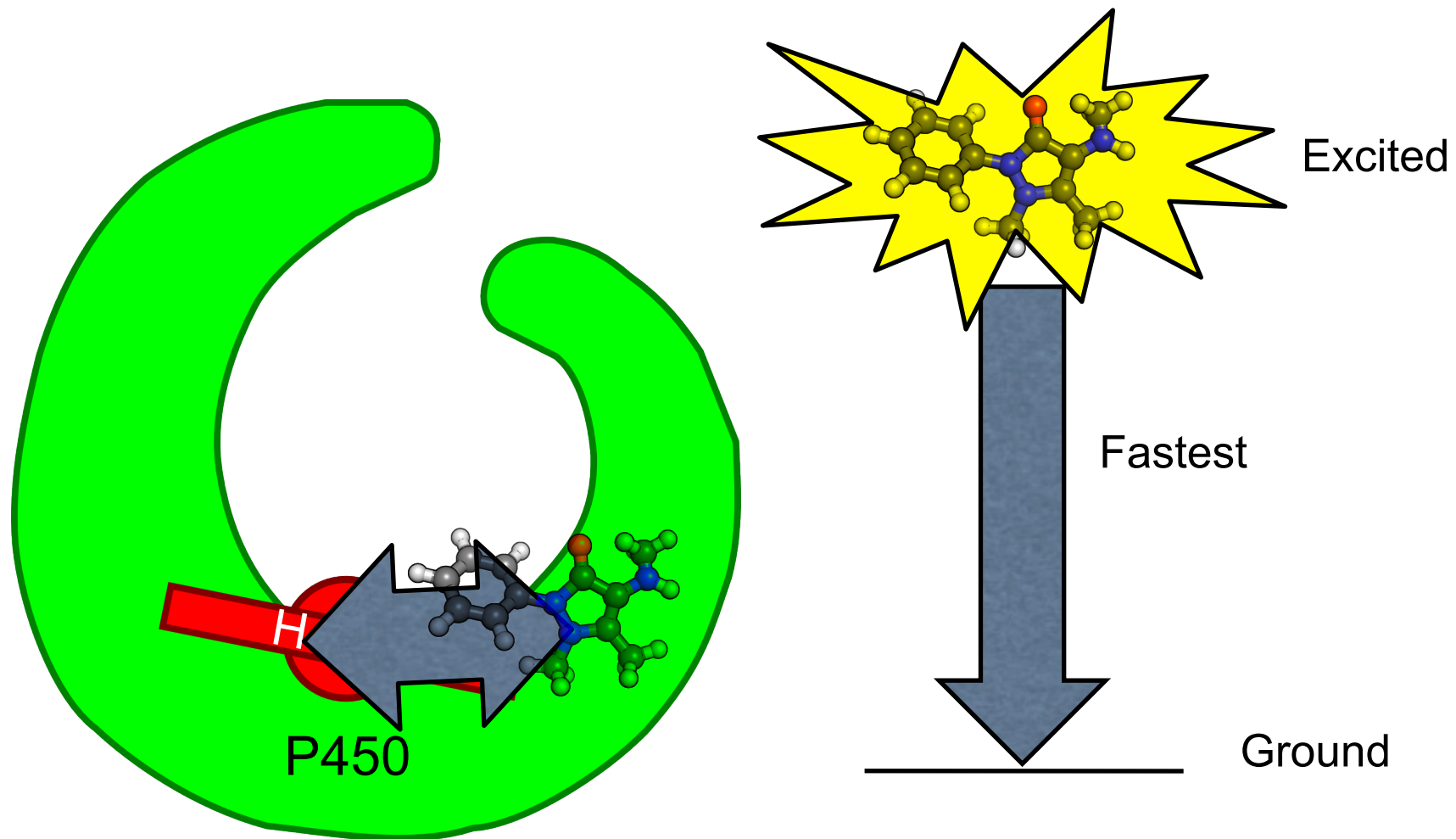
Position/Orientation: PRE NMR



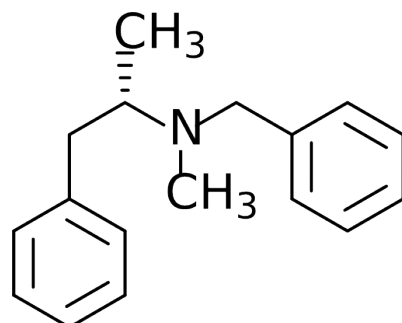
Position/Orientation: PRE NMR



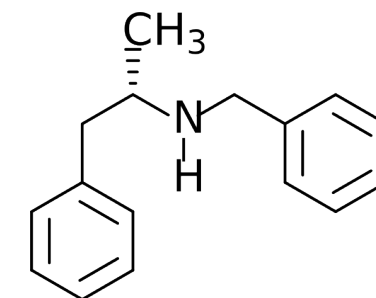
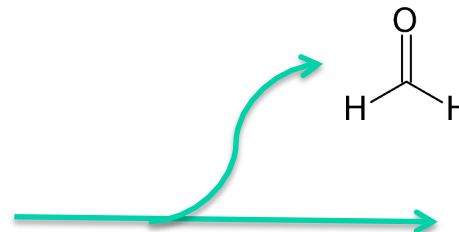
Position/Orientation: PRE NMR



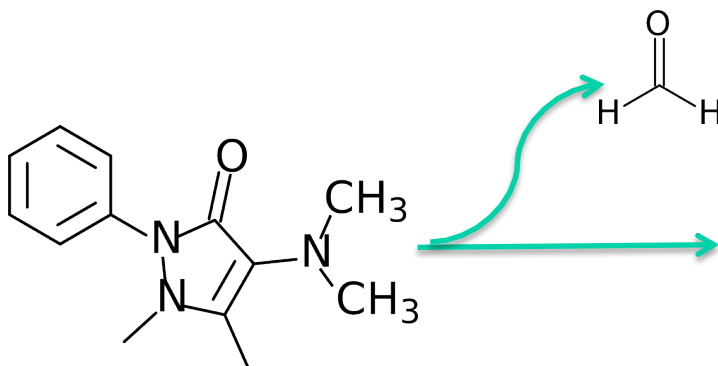
Sequential Metabolism and Cytochrome P450s



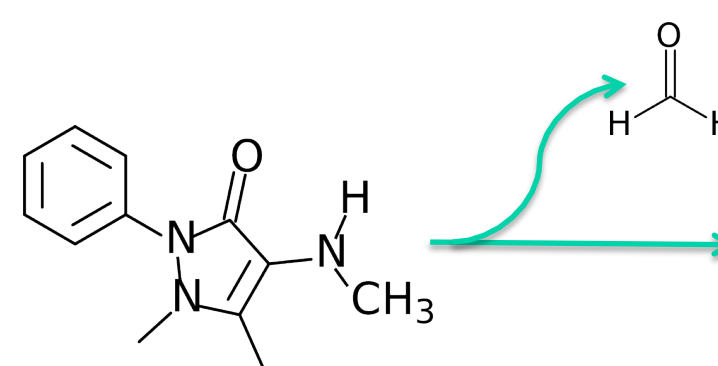
benzphetamine



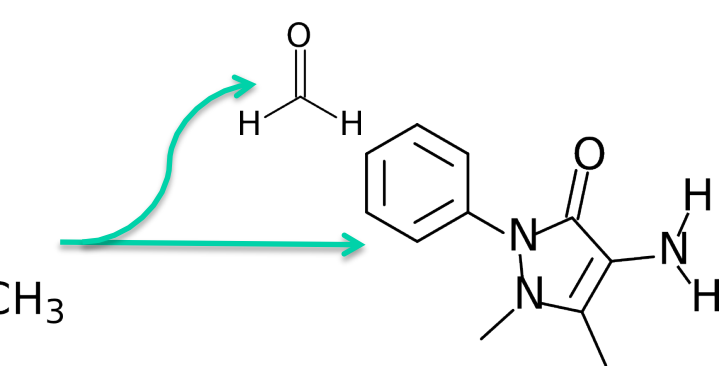
desmethylbenzphetamine



amidopyrine

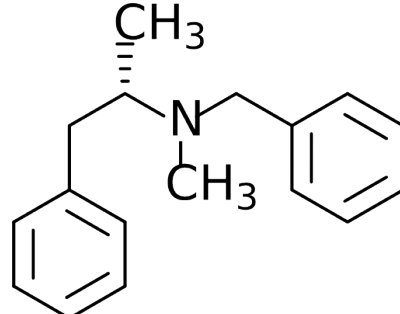


desmethylamidopyrine

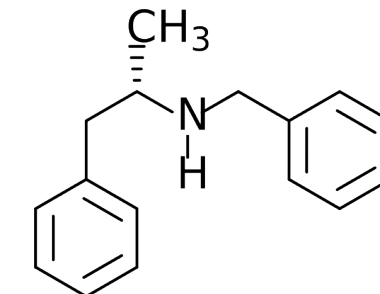
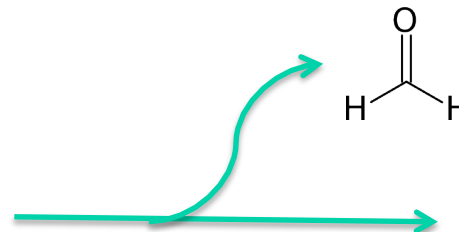


aminoantipyrine

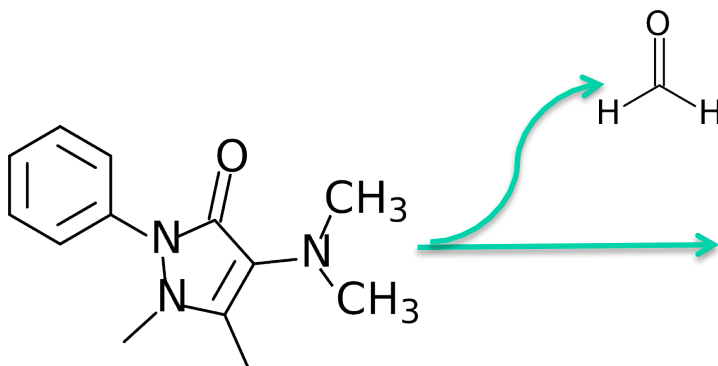
Sequential Metabolism and Cytochrome P450s



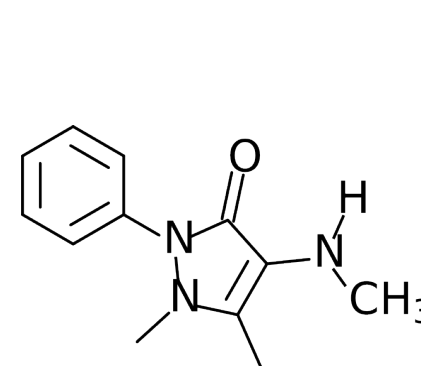
benzphetamine



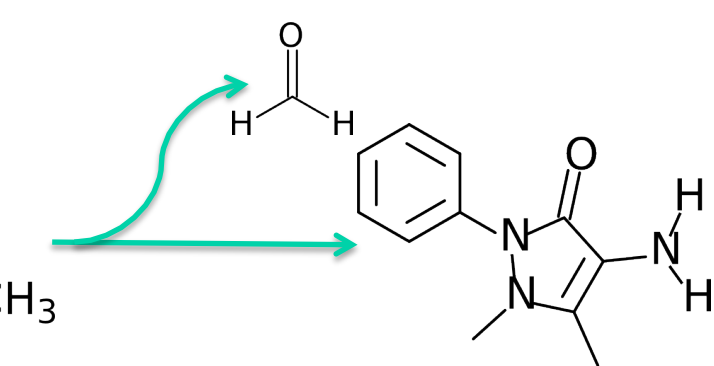
desmethylbenzphetamine



amidopyrine



desmethylamidopyrine



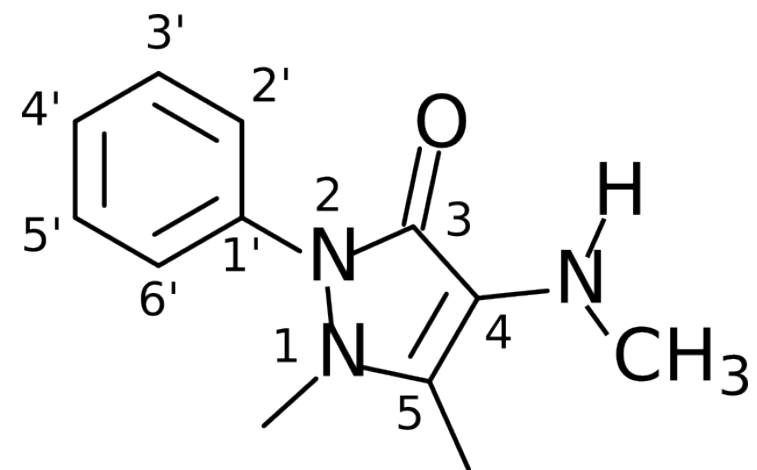
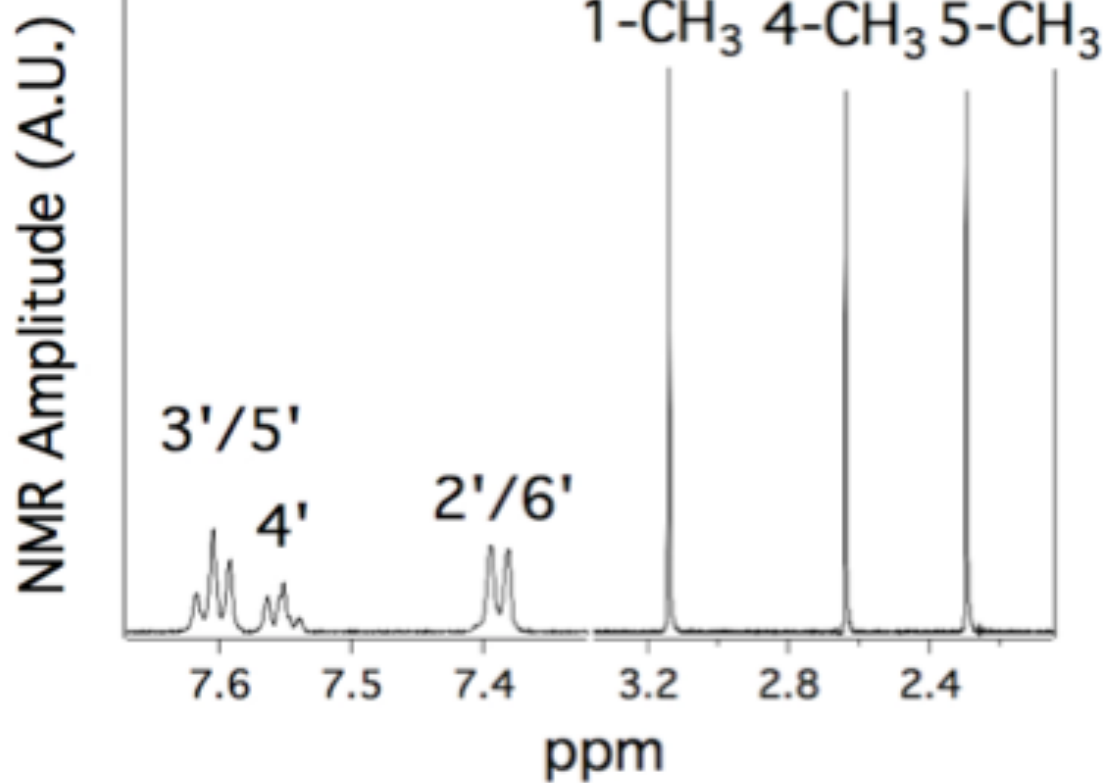
aminoantipyrine

Substrate

Intermediate

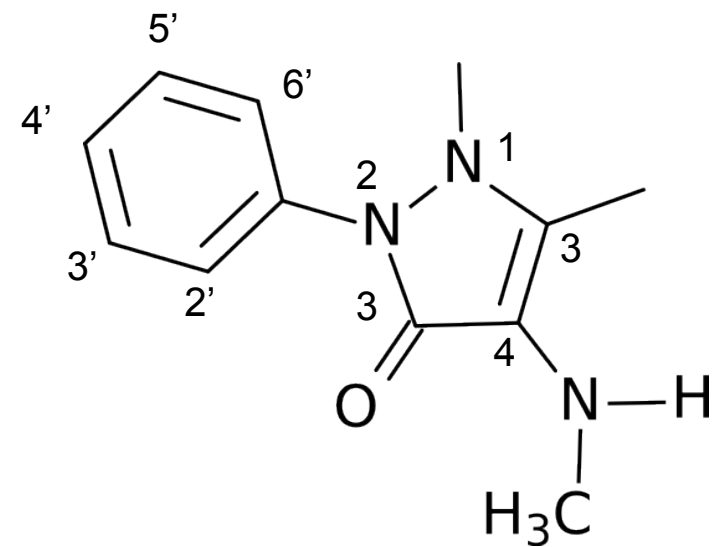
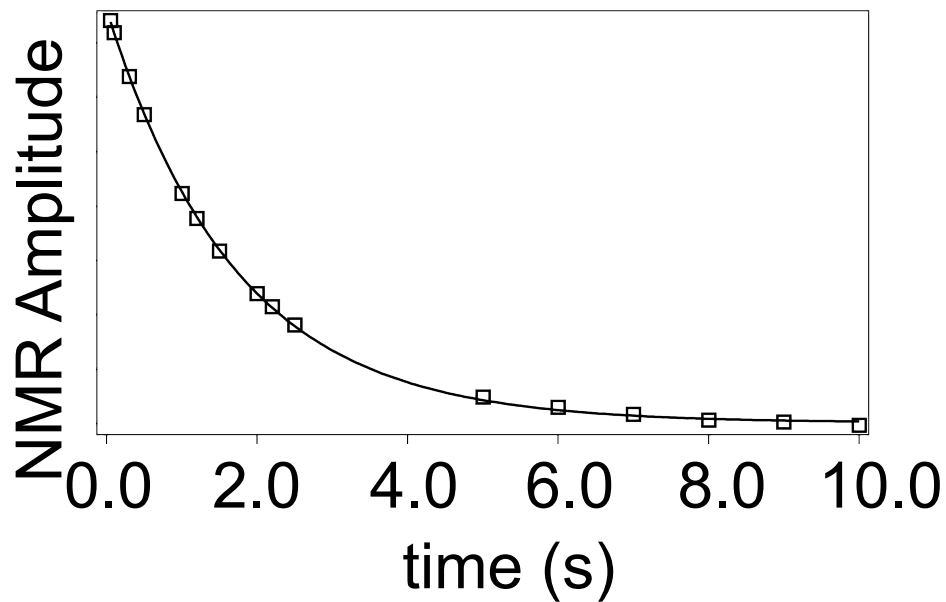
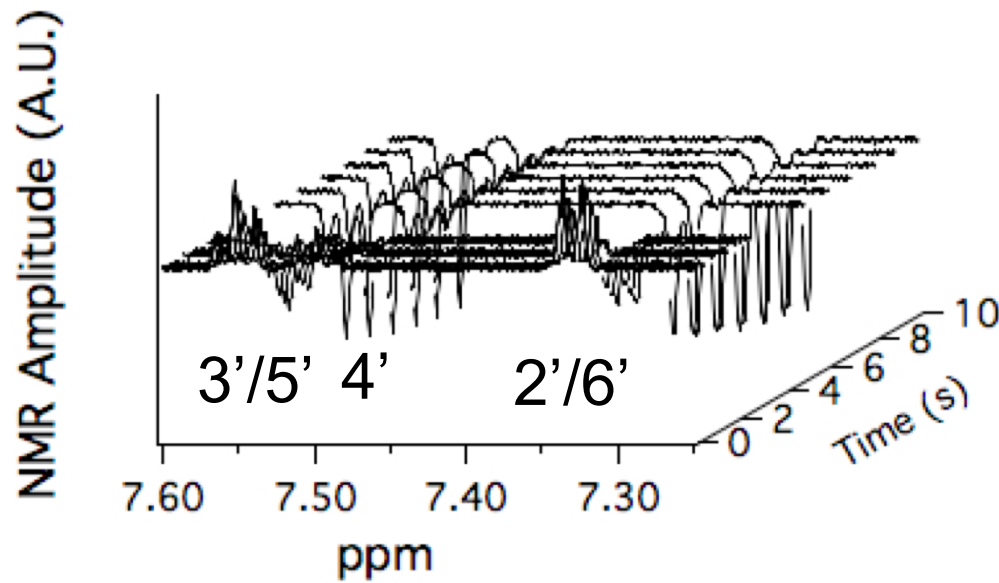
Product

NMR



desmethylamidopyrine
Intermediate

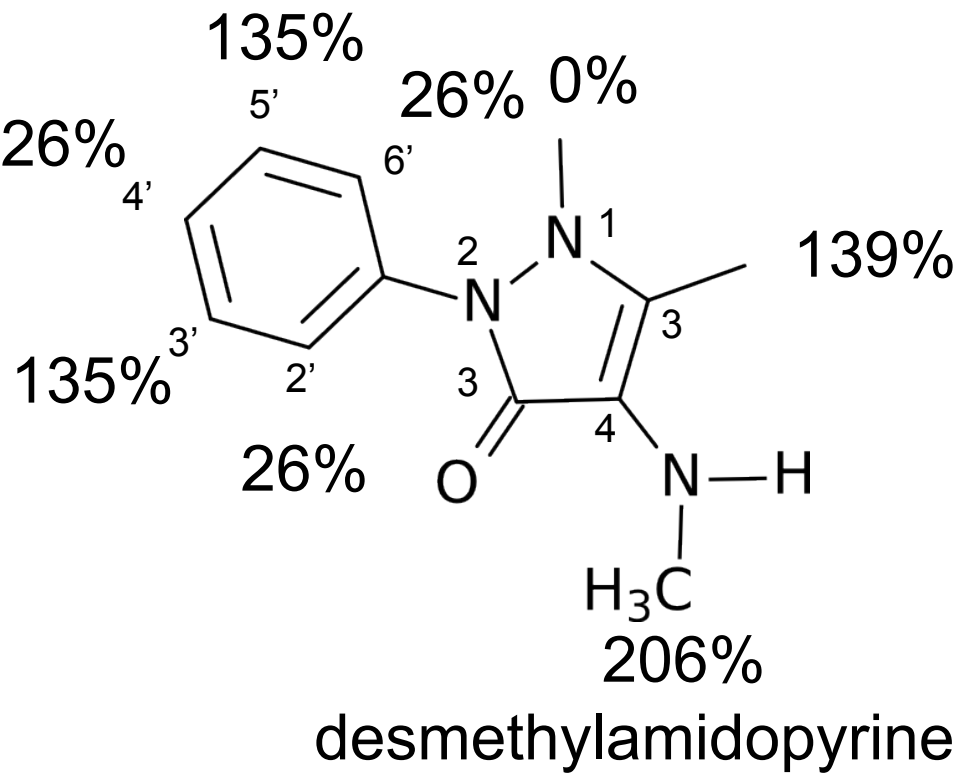
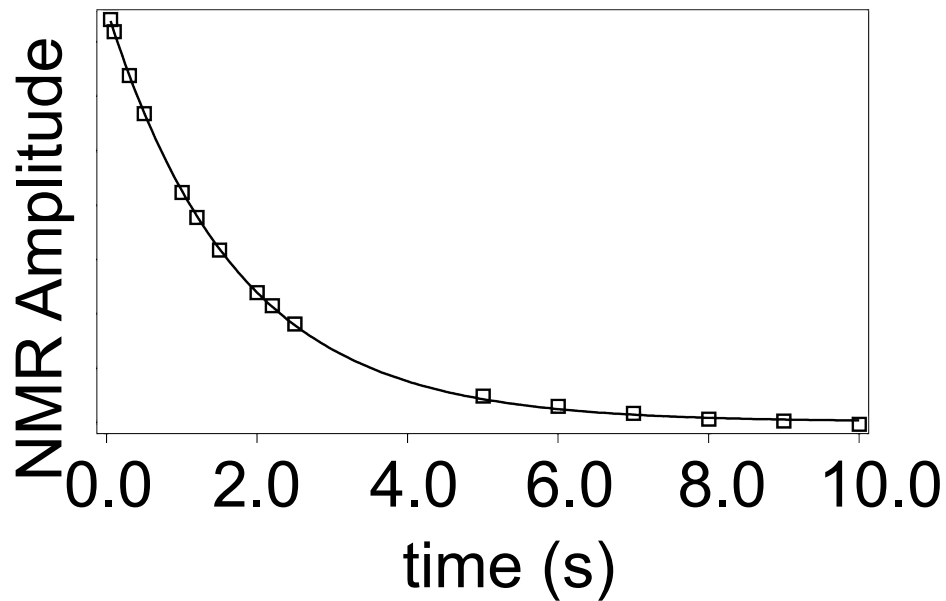
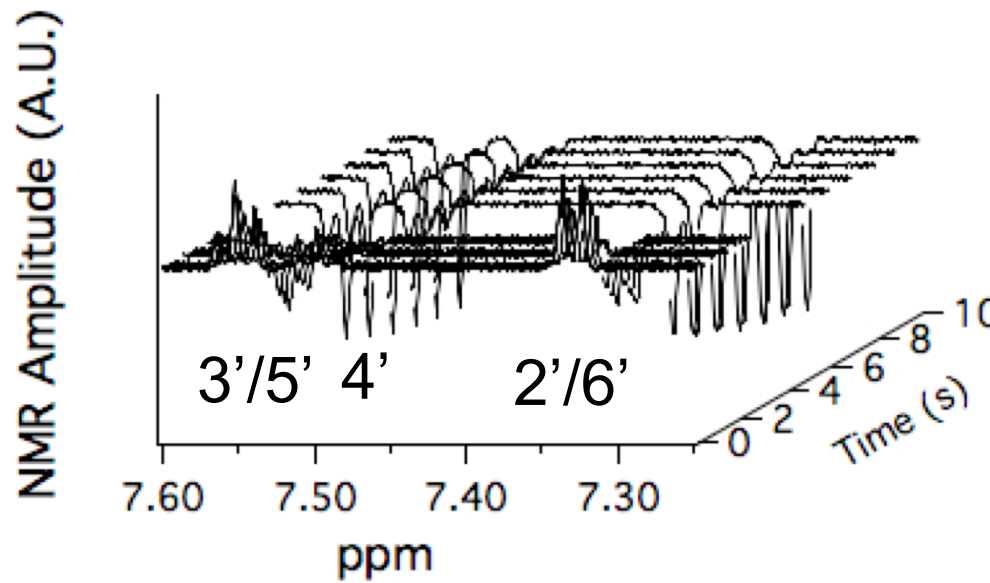
PRE NMR



desmethylamidopyrine

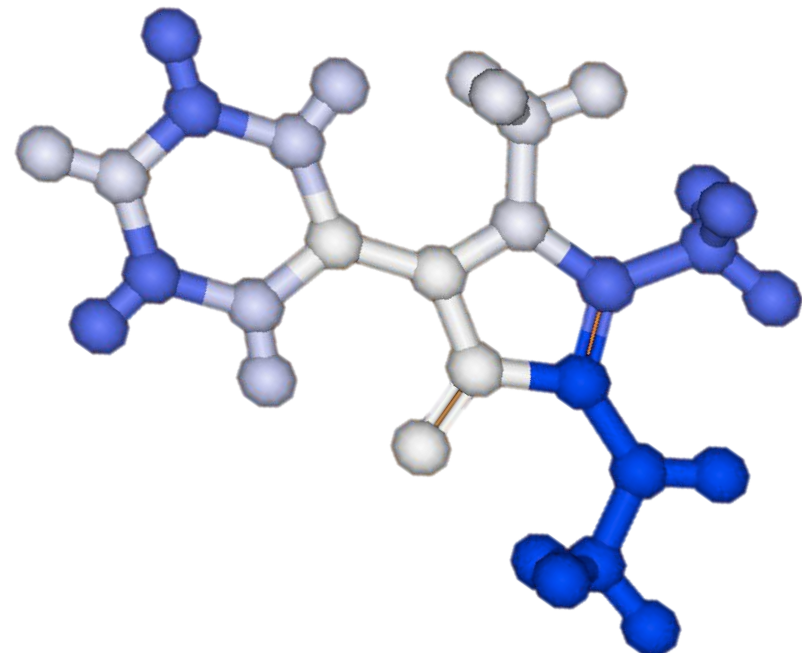
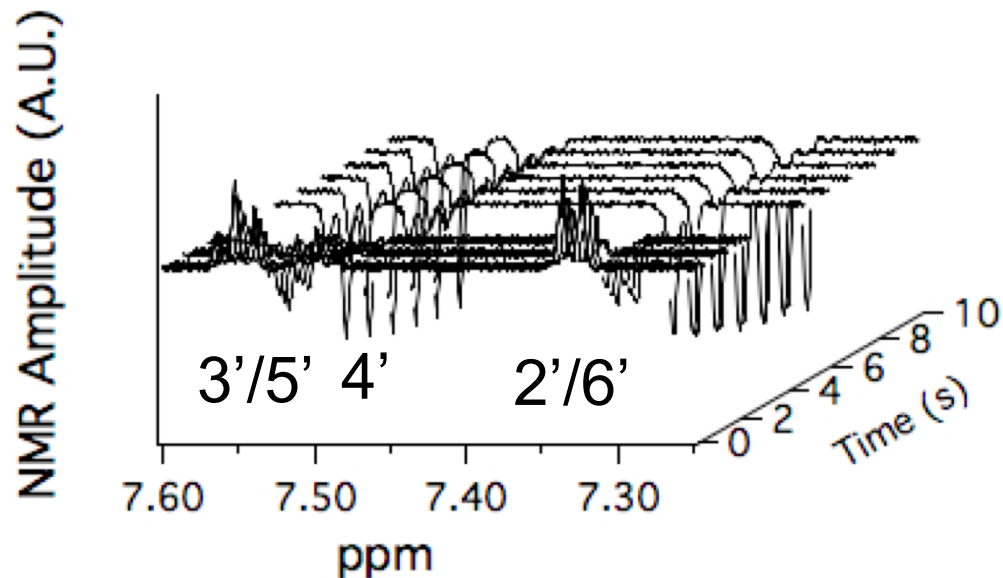
Heme

PRE NMR

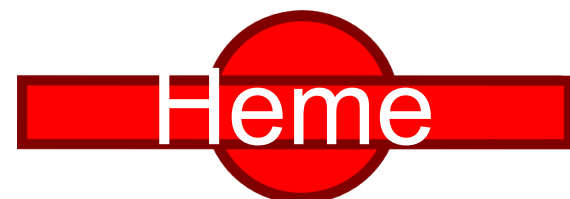
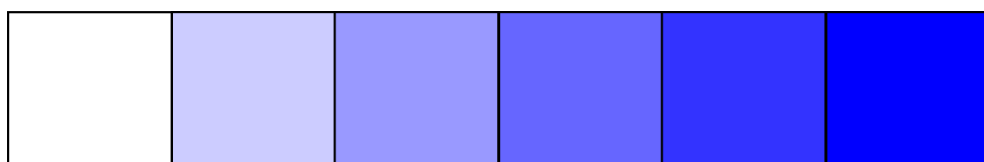


Heme

PRE NMR



desmethylamidopyrine



Farther ← → Closer

Converting Relaxation Rates into Distances

$$R_P = \frac{2}{15} \left(\frac{\mu_0}{4\pi} \right) \frac{\gamma_n^2 g_e^2 \mu_B^2 S(S+1)}{r_{app}^6} \left[\frac{\tau_c}{1 - (\omega_n - \omega_e)} + \frac{3\tau_c}{1 + \omega_n^2 \tau_c^2} + \frac{6\tau_c}{1 + (\omega_n + \omega_e)^2 \tau_c^2} \right]$$

↑
Relaxation Rate

↑
Apparent distance
Solomon-Bloembergen Equation (1955)

Converting Relaxation Rates into Distances

Constants

$$R_P = \frac{2}{15} \left(\frac{\mu_0}{4\pi} \right) \frac{\gamma_n^2 g_e^2 \mu_B^2 S(S+1)}{r_{app}^6} \left[\frac{\tau_c}{1 - (\omega_n - \omega_e)} + \frac{3\tau_c}{1 + \omega_n^2 \tau_c^2} + \frac{6\tau_c}{1 + (\omega_n + \omega_e)^2 \tau_c^2} \right]$$

Relaxation Rate

Apparent distance

Solomon-Bloembergen Equation (1955)

Converting Relaxation Rates into Distances

Constants Spin State

$$R_P = \frac{2}{15} \left(\frac{\mu_0}{4\pi} \right) \frac{\gamma_n^2 g_e^2 \mu_B^2 S(S+1)}{r_{app}^6} \left[\frac{\tau_c}{1 - (\omega_n - \omega_e)} + \frac{3\tau_c}{1 + \omega_n^2 \tau_c^2} + \frac{6\tau_c}{1 + (\omega_n + \omega_e)^2 \tau_c^2} \right]$$

Relaxation Rate

Apparent distance

Solomon-Bloembergen Equation (1955)

Converting Relaxation Rates into Distances

Constants Spin State

$$R_P = \frac{2}{15} \left(\frac{\mu_0}{4\pi} \right) \frac{\gamma_n^2 g_e^2 \mu_B^2 S(S+1)}{r_{app}^6} \left[\frac{\tau_c}{1 - (\omega_n - \omega_e)} + \frac{3\tau_c}{1 + \omega_n^2 \tau_c^2} + \frac{6\tau_c}{1 + (\omega_n + \omega_e)^2 \tau_c^2} \right]$$

R_P Apparent distance Solomon-Bloembergen Equation (1955) NMR Spectrometer Related
Relaxation Rate

Converting Relaxation Rates into Distances

Constants Spin State Correlation time nuclear-electron interaction

$$R_P = \frac{2}{15} \left(\frac{\mu_0}{4\pi} \right) \frac{\gamma_n^2 g_e^2 \mu_B^2 S(S+1)}{r_{app}^6} \left[\frac{\tau_c}{1 - (\omega_n - \omega_e)} + \frac{3\tau_c}{1 + \omega_n^2 \tau_c^2} + \frac{6\tau_c}{1 + (\omega_n + \omega_e)^2 \tau_c^2} \right]$$

Apparent distance Solomon-Bloembergen Equation (1955) NMR Spectrometer Related

Relaxation Rate

$$\frac{1}{\tau_c} = \frac{1}{\tau_s} + \frac{1}{\tau_r}$$

electronic spin relaxation

rotational time

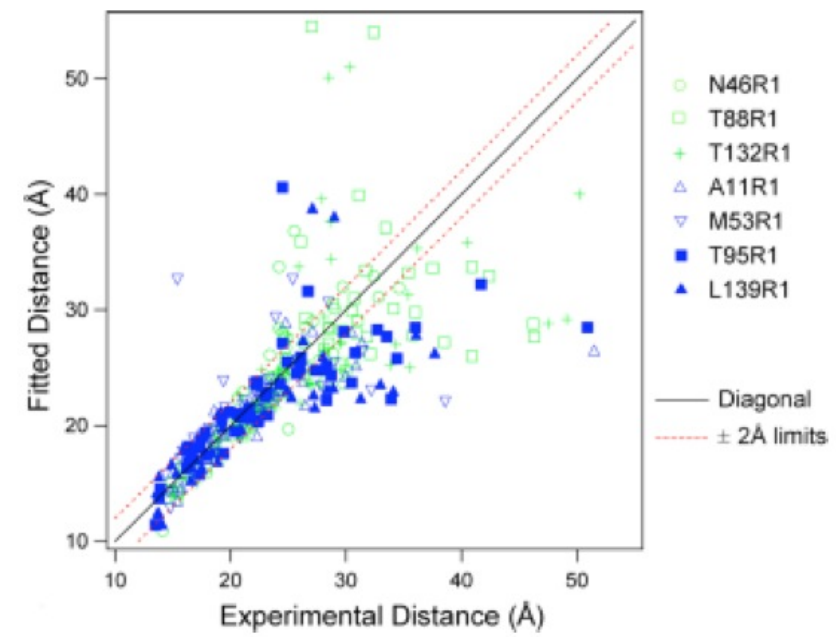
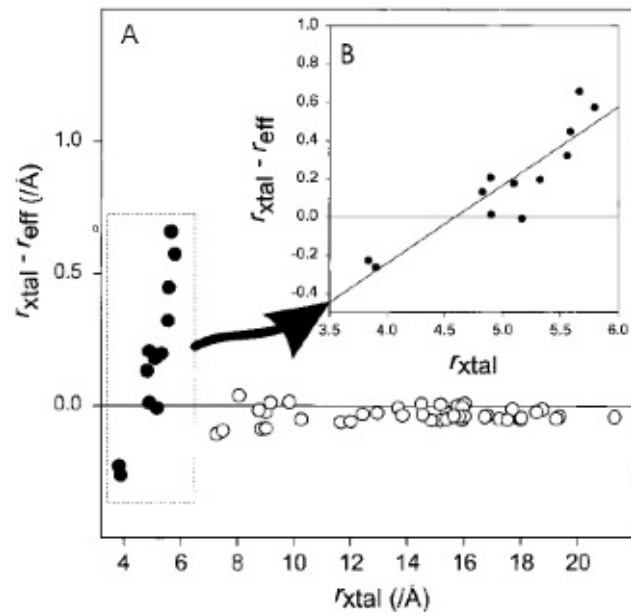
Converting Relaxation Rates into Distances- Super Simplified

$$R_P = \frac{\text{constants (Spin State)}}{r_{app}^6} \left[\frac{\text{Correlation time}}{\text{NMR Frequency}} \right]$$

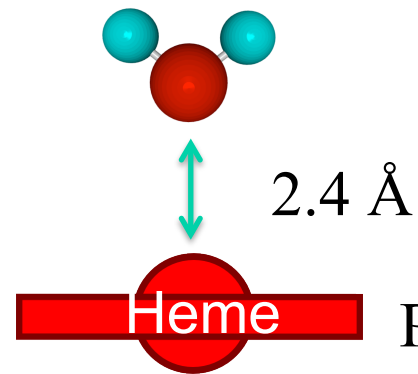
Assumptions

- Paramagnetic label (Nitroxide) relatively rigid with respect to the drug
- Electron spin relaxation not coupled to molecular tumbling
- Electronic distribution of the paramagnetic label is a point (point dipole approx)
 - Electron delocalized across the N-O
- Exchange >> Relaxation Rate

Distance Limitations?

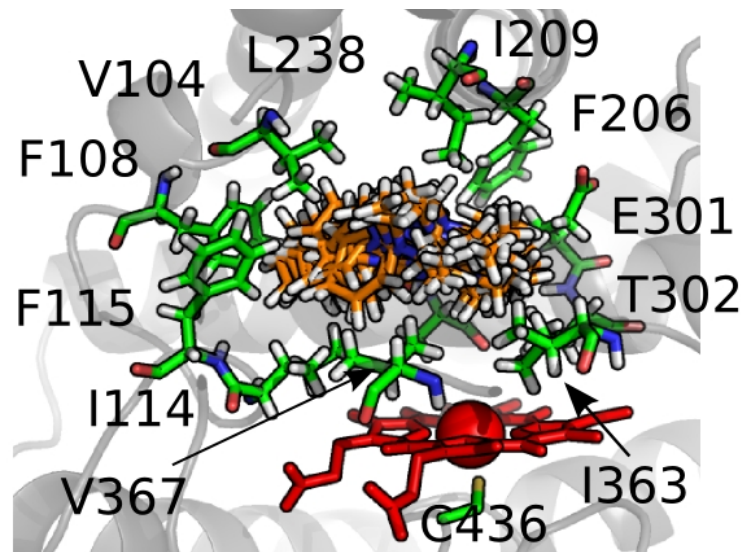


Wilkens, 1998
(Iron center
Rubredoxin)

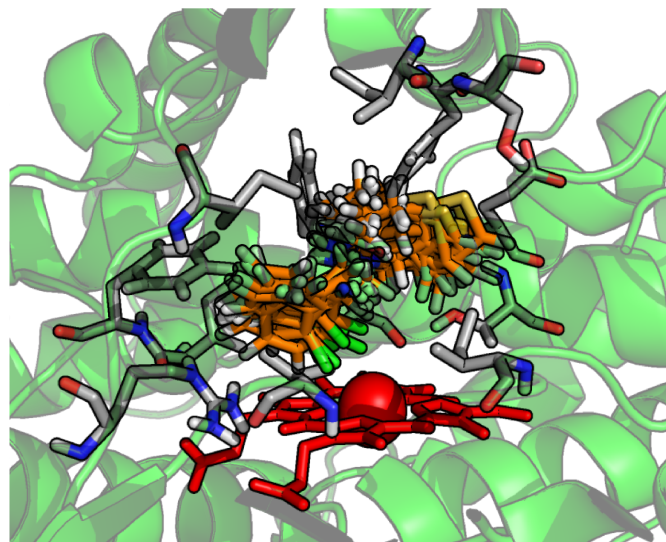


Liang, 2006 (nitroxide labeling OmpA)

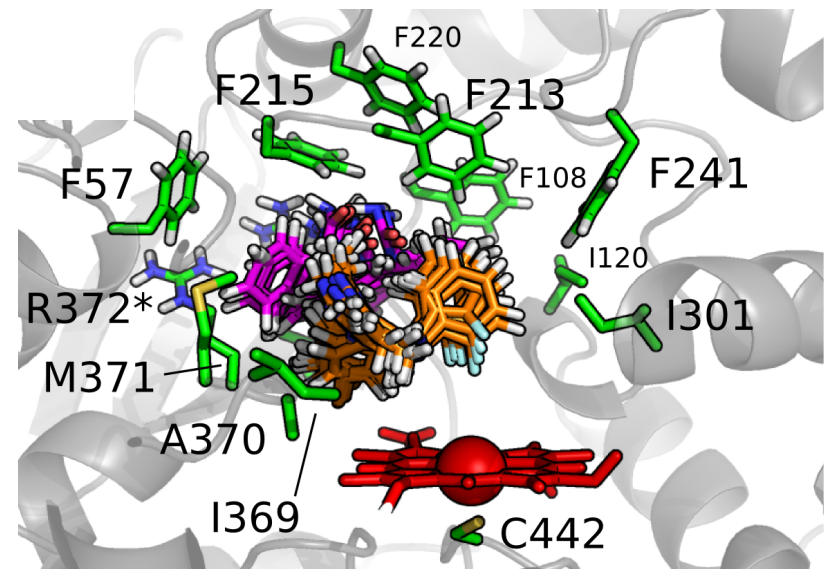
Philson, 1979 (water-P450 heme)



Sequential Metabolism

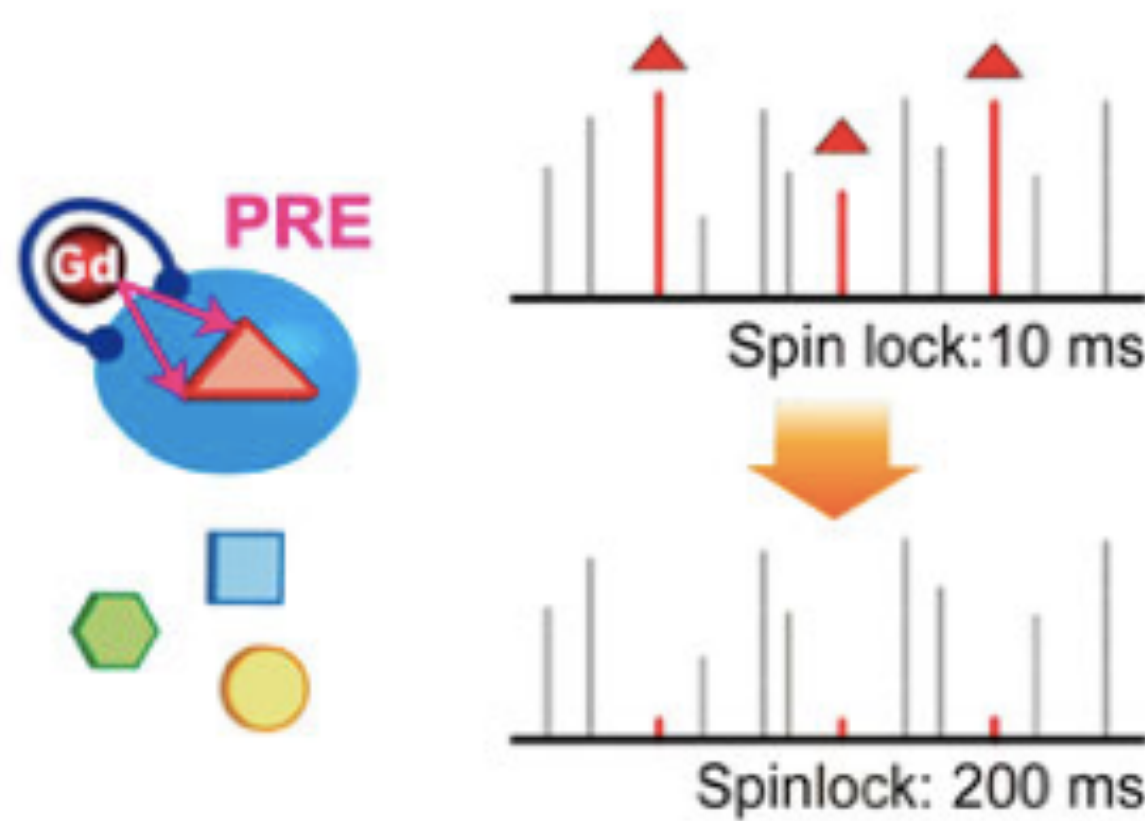


Drug Toxicity



Drug-Drug Interaction

Other: Paramagnetic Relaxation Enhancement (PRE)

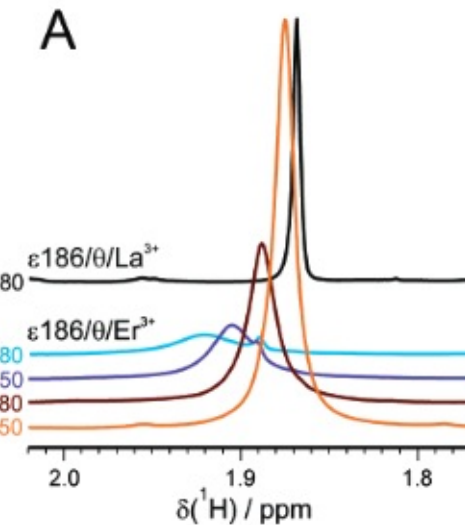
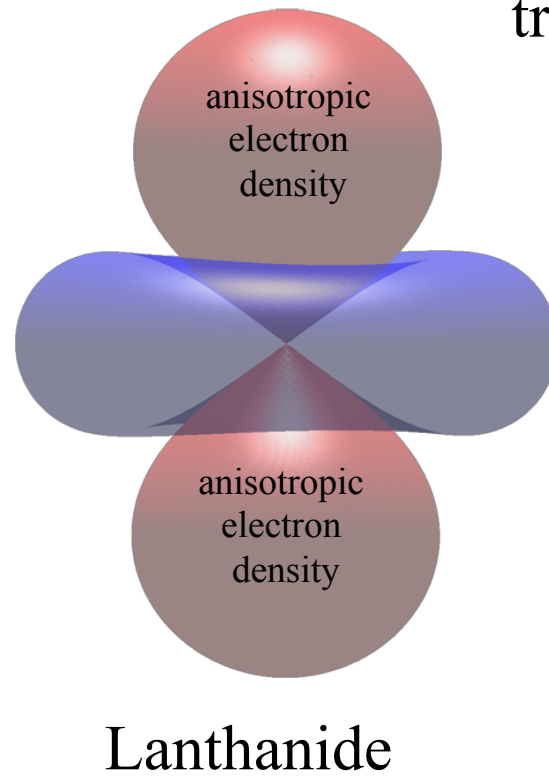


Other Methods of Ligand Based Screening

- **^{19}F -Labeling**
- **Paramagnetic Relaxation Enhancement (PRE) NMR**
- **Pseudo Contact Shift (PCS) NMR**

Other: Pseudocontact shift

transmitted through space



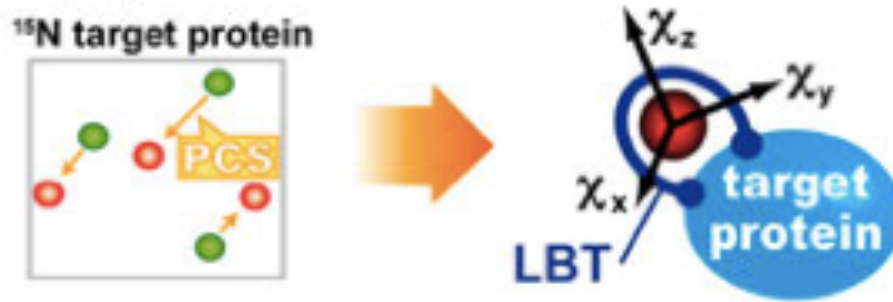
$$\delta_{pcs} = \frac{1}{12 \pi r^3} \left[\Delta\chi_{ax} (3 \cos^2 \theta - 1) + \frac{3}{2} \Delta\chi_{rh} (\sin^2 \theta \cos 2\phi) \right]$$

Lanthanides															V·T·E
Lanthanum	Cerium	Praseo-dymium	Neodymium	Promethium	Samarium	Europium	Gadolinium	Terbium	Dysprosium	Holmium	Erbium	Thulium	Ytterbium	Lutetium	
57 La	58 Ce	59 Pr	60 Nd	61 Pm	62 Sm	63 Eu	64 Gd	65 Tb	66 Dy	67 Ho	68 Er	69 Tm	70 Yb	71 Lu	

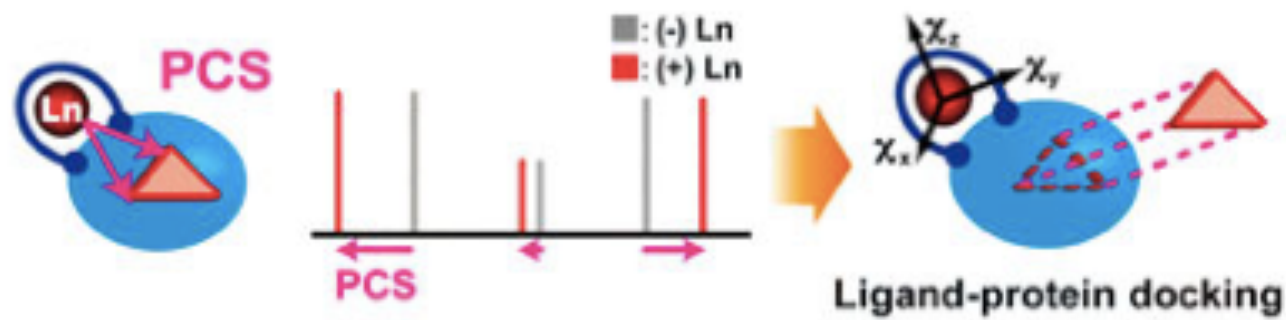
John, M.; Pintacuda, G.; Park, A. Y.; Dixon, N. E.; Otting, G., *JACS* **2006**, 128, (39), 12910-12916.

Other: Pseudo Contact Shift (PCS)

(i) $\Delta\chi$ -tensor determination



(ii) Structure determination



Summary

	SAR by NMR	STD NMR	Spin labeling	Diffusion editing	Inverse NOE Pumping	Water-LOGSY
Large protein (> 30 kDa)	limited ^[a]	yes	yes	no	yes	yes
small protein (< 10 kDa)	yes	no	yes	yes	no	no
Isotope-labeled protein required	yes	no	no	no	no	no
Binding epitope on protein	yes ^[d]	no	no	no	no	no
Binding epitope on ligand	no	yes	no	no	yes ^[d]	yes ^[e]
Amount of protein [nmol] at 500 MHz	25	0.1	~1	~100	~25	~25
K_D tight binding	no limit	100 pm	100 pm	~100 nM	1 nM	100 pm
K_D weak binding	~1 mM	~10 mM	~10 mM	~1 mM	~1 mM	~10 mM
Identification of ligand	no	yes	yes	yes	yes	yes
Comments	robust method	robust method	sensitive method, but results ambiguous if lysine positions unknown	relatively insensitive method	stable method, but ligand excess and mixing time need to be optimized	good for very hydrophilic targets and/or ligands

[a] TROSY necessary. [b] But chemical modification. [c] If protein is assigned. [d] Not realized. [e] But water contact surface.

Figure 2 | Trends in the application of fragment-based screening. The number of industrial (blue diamonds) and academic groups (green squares) that have used fragment-based screening as part of their lead generation strategies (based on publications and/or conference materials) as a function of time.

Is FBDD Working?

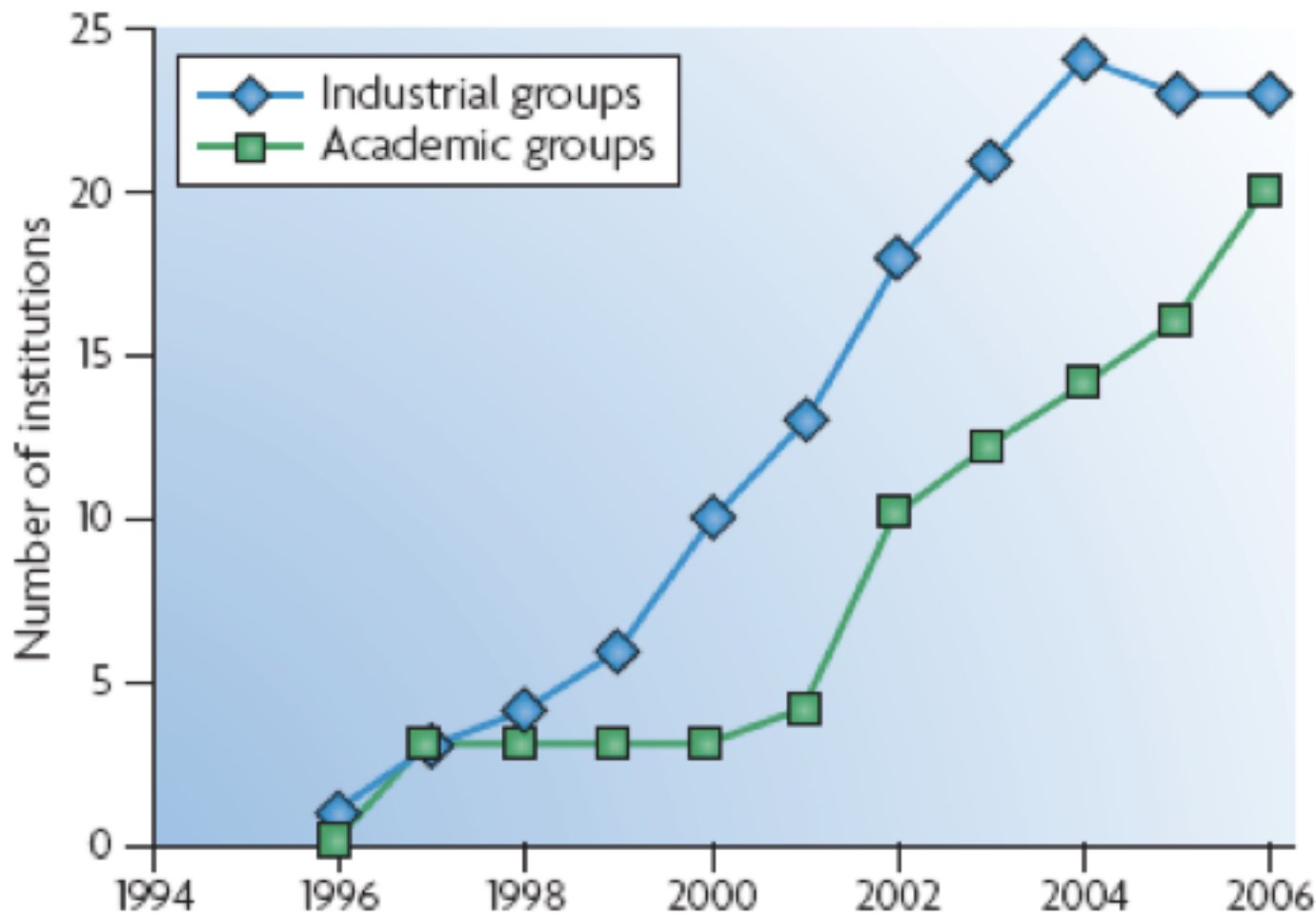
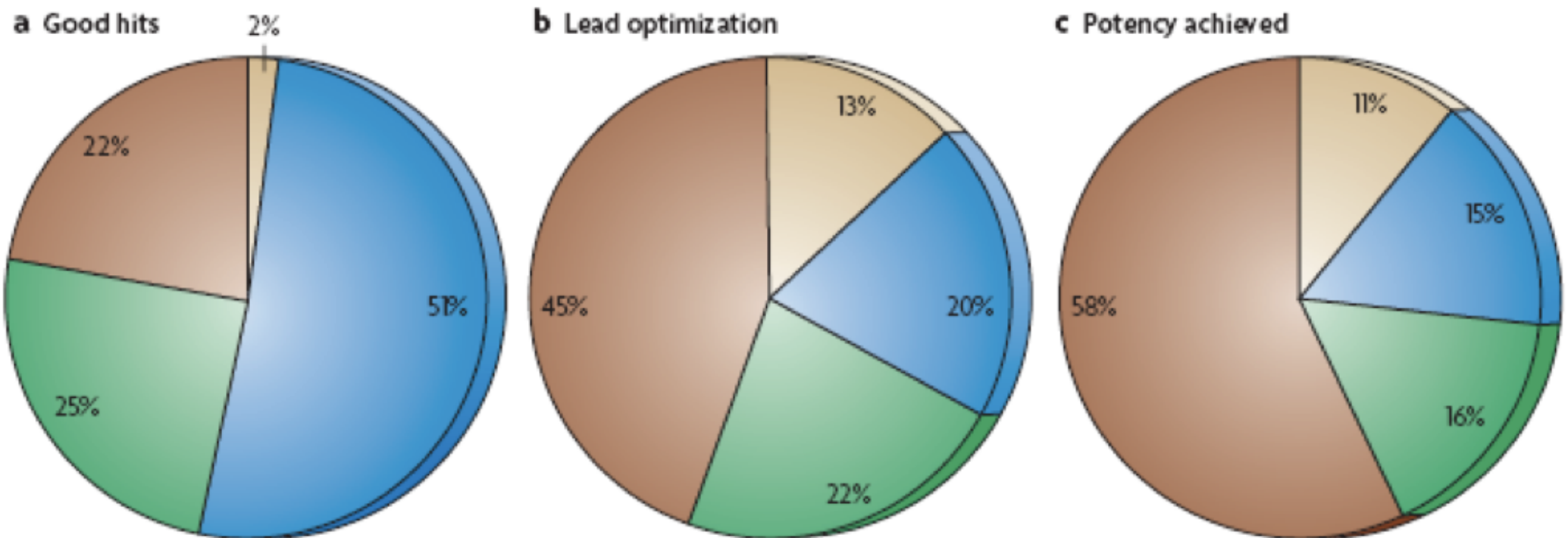


Figure 4 | Comparing high-throughput screening and fragment-based screening. This figure shows the percentage of a set of 45 protein targets that underwent both high-throughput screening (HTS) and fragment-based screening (FBS) and reached critical discovery milestones: (a) Chemically tractable hits; (b) Lead optimization initiated around hits from the specified lead source; (c) Potency (defined as $IC_{50} < 100$ nM) achieved from the specified lead source.

Is FBDD Working?



High Throughput Screening (HTS)



Fragment Based Drug Design (FBDD)



Both



Neither

Company	Target	Endpoint
Abbott	Matrix metalloproteinase (MMP) ¹⁸	Phase I (ABT-518)
Abbott	B-cell CLL/lymphoma 2 (BCL-2), BCL-2-like 1 (BCL-XL) ¹⁹	Preclinical development (ABT-737)
Abbott	FK506-binding protein (FKBP) ¹⁵	Novel, potent inhibitors
Abbott	Leukocyte function-associated antigen-1 (LFA) ⁵⁹	Novel, potent inhibitors
Abbott	Protein tyrosine phosphatase-1B (PTP1B) ⁶⁰	Novel, potent inhibitors
Abbott	Dihydronopterin aldolase (DHNA) ⁶¹	Novel, potent inhibitors
Abbott	BCL-2 selective	Novel, potent inhibitors
Abbott	Heat shock protein-90 (HSP90)	Novel, potent inhibitors
Abbott	Survivin	Novel, potent inhibitors
Abbott	Poly(ADP-ribose) polymerase (PARP)	Novel, potent inhibitors
Abbott	Methionine aminopeptidase-2 (MetAP2)	Novel, potent inhibitors
Abbott	Casein kinase-2 (CK2)	Novel, potent inhibitors
Abbott	Kinase insert domain receptor (KDR)	Novel, potent inhibitors
Abbott	v-akt murine thymoma viral oncogene homolog-1 (AKT-1)	Novel, potent inhibitors
Astex Therapeutics	Aurora kinase ⁶²	Phase I (AT9283)
Astex Therapeutics	Cyclin-dependent kinase (CDK) ⁶²	Phase I (AT7519)
Astex Therapeutics	CDK ⁶²	Preclinical development (AT9311)
Astex Therapeutics	HSP90 ⁶²	Preclinical development (AT13387)
Astex Therapeutics	Mitogen-activated protein kinase-14 (P38 α) ⁶³	Novel, potent inhibitors
Aventis	Src SH2 domain ^{64,65}	Novel, potent inhibitors
Burnham Institute	Anthrax lethal factor ⁶⁶	Novel, potent inhibitors
Novartis	3 α -hydroxysteroid dehydrogenase (3 α -HSD)	Novel, potent inhibitors
Plexxikon	Peroxisome proliferator-activated receptor (PPAR) (Metabolic)	Phase II (PPM204)
Plexxikon	Oncogenic v-raf murine sarcoma viral oncogene homolog B1 (B-Raf)	Investigational new drug application (PLX4032)
Plexxikon	PPAR multiple sclerosis	Preclinical development